THE $T(\alpha, \gamma)Li^7$ REACTION AND A STANDARD GEIGER-MULLER COUNTER FOR GAMMA RAY FLUX DETERMINATIONS

by

RICHARD ALEXANDER MORROW

B.Sc., Queen's University, 1958

A THESIS SUBMITTED IN PARTIAL FULFILMENT OF

THE REQUIREMENTS FOR THE DEGREE OF

MASTER OF SCIENCE

in the Department

of

PHYSICS

We accept this thesis as conforming to the

required standard

THE UNIVERSITY OF BRITISH COLUMBIA

September 1959

ABSTRACT

A study of the $T(\alpha,\gamma)Li^7$ reaction has been made at mean alpha particle energies of 1320, 560 and 350 Kev in a solid tritium-zirconium target. At the 1320 Kev energy the absolute 90° differential cross-section for transitions to the ground state has been found to be 1.89×10^{-31} cm^2 per steradian from analyses of spectra obtained in a $2\frac{3}{4}" \times 4\frac{1}{2}"$ NaI crystal. At this energy the ratio of the differential cross-section for transitions to the first excited state to that for transitions to the ground state was found to be 0.446. This ratio was observed to remain the same at all detector angles. The excitation function roughly determined by additional runs at 560 and 350 Kev mean energy followed the form obtained by Riley of this laboratory in 1958.

Angular distribution measurements at 1320 Kev gave the result that both the above mentioned gamma rays have the same angular dependence, this being $1-0.11 \cos^2\theta + 0.39 \cos^4\theta$. At 560 Kev mean energy their anisotropy was measured to be about 5%.

A background from the target has been found to have an angular distribution at 1320 Kev mean alpha particle energy of $1+0.35 \cos\theta$ in laboratory co-ordinates. Both its excitation function, determined roughly from runs at 560 and 350 Kev, and its anisotropy followed a form in agreement with neutron counter measurements. It is suggested that this background is caused by neutrons from some still unknown reaction in the target.

An investigation was also made of a standard thick-walled brass Geiger-Muller counter to determine its efficiency for photon energies from 0.5 to 20 Mev. A smooth curve was obtained showing efficiency increasing with gamma ray energy thus agreeing in form with previous experimental and theoretical results.

In presenting this thesis in partial fulfilment of the requirements for an advanced degree at the University of British Columbia, I agree that the Library shall make it freely available for reference and study. I further agree that permission for extensive copying of this thesis for scholarly purposes may be granted by the Head of my Department or by his representatives. It is understood that copying or publication of this thesis for financial gain shall not be allowed without my written permission.

Department of Physics

The University of British Columbia,
Vancouver 8, Canada.

Date September 12, 1959

ACKNOWLEDGEMENTS

The author wishes to thank Dr. G.M. Griffiths for suggesting this research and for his help and encouragement in carrying it out.

Thanks are also extended to Mr. P.P. Singh whose assistance in much of the experimentation was invaluable.

A National Research Council of Canada Bursary which made this work possible is gratefully acknowledged.

TABLE OF CONTENTS

CHAPTER		PAGE
	Part I The $T(\alpha,\gamma)Li^7$ Reaction	
I	Introduction	1
II	Experimental	6
	1. Apparatus:	6
	(a) Van de Graaff Generator	6
	(b) Sidearm Arrangement	7
	(c) Scintillation Counter	8
	(i) Shielding	8
	(ii) Efficiency	9
	(d) Electronics	12
	2. Tritium Target	12
	(a) Mounting	12
	(b) Tritium Content	13
	(i) β-activity	13
	(ii) $T(p,\gamma)He^4$ Yield	14
	(c) Thickness for Alpha Particles	17
	3. Angular Distribution Measurements	18
	(a) Procedure	18
	(b) Standard Gamma Ray Spectrum	21
	(c) $T(\alpha,\gamma)Li^7$ Spectra	22
	(d) Branching Ratios	24
	(e) Angular Distribution	25
	(f) Doppler Shift	28
	4. Backgrounds:	29
	(a) General	29
	(b) Energy of Neutrons	30
	(c) Yield and Anisotropy of Neutrons	31
	(d) Background Yield from the Scintillation Counter	32
	(e) Angular Distribution	33
	5. Absolute 90° Differential Cross-Section	34
	(a) Procedure	34
	(b) Cross-Section at 1.6 Mev	35
	(c) Excitation Function	36
	(d) Target Thickness from Gamma Ray Energy	38
	6. Summary and Discussion of Experimental Results	38

CHAPTER		PAGE
II	7. Application of Results to Astrophysics ..	40
	Part II A Standard Geiger-Muller Counter for Gamma Ray Flux Determinations	
I	Introduction	44
II	Determination of Characteristics	48
	1. Method of Operation	48
	2. Construction and Filling	49
	3. Plateaux and Resolving Time	51
	4. G-M Counter Efficiency Determination	52
	(a) Definition of Efficiency	52
	(b) Experimental Procedure	54
	(c) Procedure at 0.51 Mev	55
	(d) " " 1.25 Mev	56
	(e) " " 6.16 Mev	57
	(f) " " 12.1 Mev	58
	(g) " " 16.3 Mev	60
	(h) " " 20.3 Mev	61
	(i) Summary of Efficiency Results	62
Bibliography		64

ILLUSTRATIONS

FIGURE NUMBER	SUBJECT	FACING PAGE
1.	Low Energy Levels of Li^7	1
2.	Sidearm Arrangement	7
3.	Scintillation Counter Efficiency	9
4.	Block Diagram of Electronics	12
5.	20 Mev $T(p,\gamma)He^4$ Spectrum	14
6.	Gamma Ray Absorption Factor for Target Backing	15
7.	Stopping Cross Sections in Zirconium-tritium Target	16
8.	Target Thickness for Alpha Particles	18
9.	$T(\alpha,\gamma)Li^7$ Spectra	21
10.	Standard Gamma Ray Spectrum	22
11.	Decomposition of $T(\alpha,\gamma)Li^7$ Spectrum	23
12.	$T(\alpha,\gamma)Li^7$ Angular Distribution	24
13.	Angular Distribution at 1.6 Mev	27
14.	Neutron Spectra	31
15.	Cross-section Factor, S	41
16.	Standard G-M Counter	49
17.	Counter Filling System	50
18.	Circuit Connections	54
19.	Co^{60} and Na^{22} Spectra	55
20.	Spectra of $B^{11}(p,\gamma)C^{12}$ Gamma Rays	59
21.	Spectra of $Li^7(p,\gamma)Be^8$ Gamma Rays	60
22.	G-M Counter Efficiency	62

FIGURE I LOW ENERGY LEVELS OF Li^7

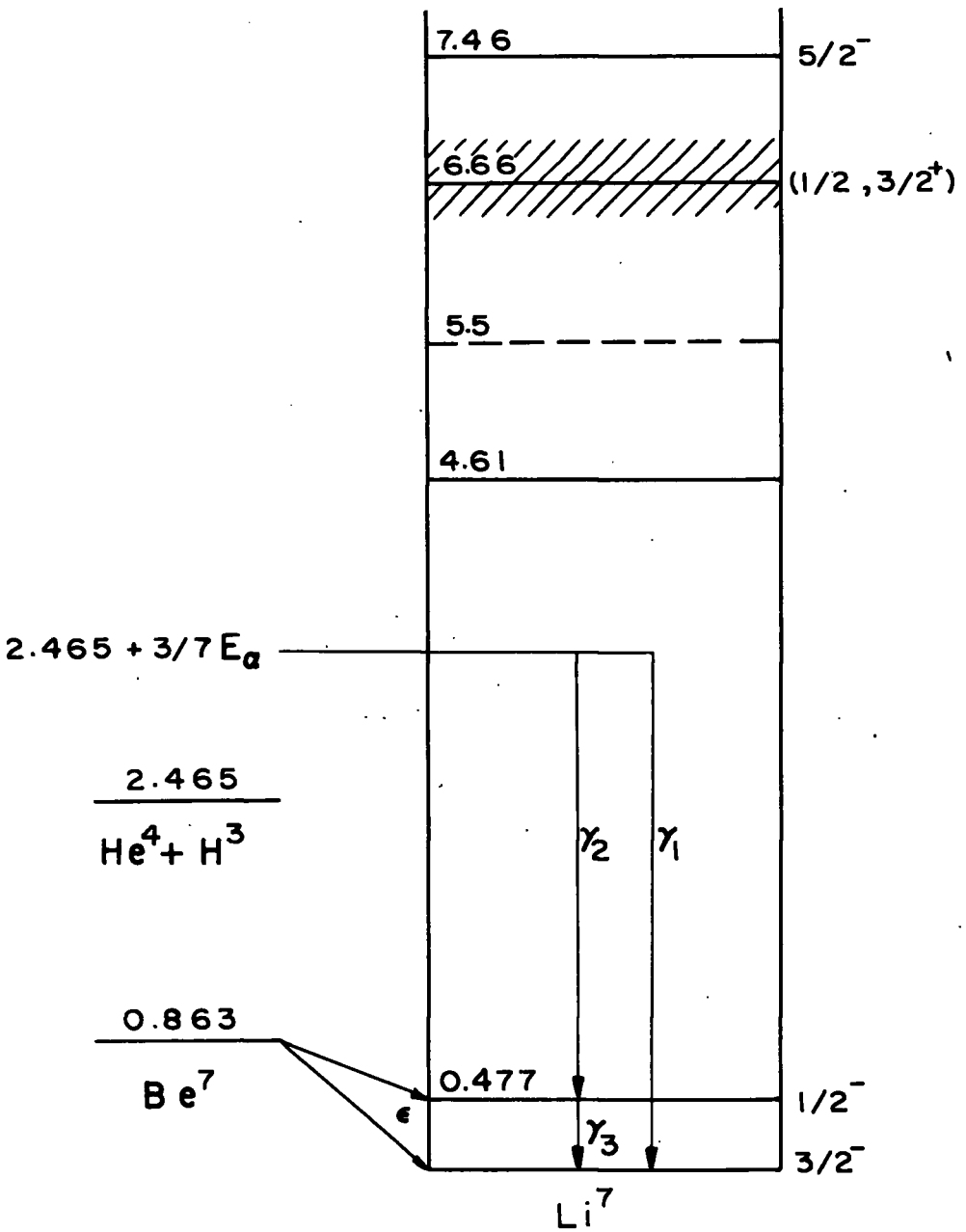

THE T (α, γ) Li^7 REACTION

Chapter I

Introduction:

In recent years there has been considerable interest in the mass 7 nuclei Li^7 and Be^7 both because of their astrophysical importance and because of considerable interest in the nature of the coupling responsible for the energy levels. Much of this interest has been concerned with the ground state and first excited state properties of these nuclei and in this connection a puzzling point is the relatively small excitation energy of about one-half Mev of the first excited states of both these nuclei as compared with about two Mev in surrounding ones.

According to simple shell model theory the two neutrons in the p-shell of Li^7 couple their angular momenta and spins to zero so that the properties of the two lower states are determined by the odd p-shell proton. This should result in the ground state being a $^2P_{3/2}$ level and the first excited state a $^2P_{1/2}$ level. The situation in the mirror nucleus Be^7 is similar in that the roles of the neutrons and protons are simply interchanged resulting in the same lower level designations as in Li^7.

From experimental observations it is indeed verified that the ground state of Li^7 is a J=3/2 level with odd parity

(Breit and Stehn, 1938). Experiments on the angular correlation of γ-rays and α-particles from $B^{10}(n,\alpha)Li^7$ (Rose and Wilson, 1950), γ-rays and α-particles from $Be^9(d,\alpha)Li^7$, and γ-ra ys and protons from $Li^6(d,p)Li^7$ (Ajzenberg and Lauritsen 1955) show isotropy as do measurements on the 0.478 Mev γ-ray from $Li^7(p,p^1)Li^{7*}$ (Littauer, 1950) thus pointing to the assignment of J=1/2 to the first excited state. However, such a choice is inconsistent with the observed ratios of intensities of β rays from Be^7 and α-particles from $B^{10}(n,\alpha)Li^7$ to the first two levels of Li^7. A J=5/2 designation would be necessary to explain these latter observations (Hanna and Inglis, 1949). Since magnetic dipole radiation would be emitted in the de-excitation of the first level with either a J=5/2 or J=1/2 assignment no differentiation could be made from lifetime measurements of Li^{7*}. The mean lifetime has been measured, however, by a number of experimenters (Ajzenberg and Lauritsen, 1955) to be about 10^{-13} second which is consistent with a magnetic dipole transition.

In the case of Be^7, unstable by K capture to Li^7 by 0.863 Mev with a half-life of 53 days, the negative results of the reaction $He^4(\alpha,n)Be^7$ support the assumption that this nucleus has odd parity (Ajzenberg and Lauritsen, 1955). From stripping theory applied to $Li^6(d,n)Be^7$ the ground state of Be^7 is again indicated to have odd parity and to have $J \leq 5/2$. Ob-

servations on the anisotropy of the neutrons with respect to the deuteron beam at E_d=0.60 Mev. and the gamma ray isotropy with respect to the neutrons definitely indicated that the 0.43 Mev excited level of Be^7 has J=1/2. The superallowed nature of the β decay $Be^7(\epsilon)Li^{7*}$ limits the ground state of Be^7 to have $J \leq 3/2$. A value of about 10^{-13} second for the half-life of the J=1/2 level of Be^7 is in agreement with the supposition that this decay occurs by magnetic dipole emission.

It would therefore appear that the single particle picture of these nuclei does give a qualitative picture of the two lowest levels but is not sufficient for a quantitative description of all features.

Apart from the interest in the ground states of the mass 7 nuclei there is great interest in the formation of these nuclei in astrophysics from the standpoint of explaining quantitatively the p-p chain in hydrogen-burning stars (Fowler, 1958). In this process four hydrogen atoms are converted to one helium atom accompanied by the release of 26.7 Mev of energy. The possible processes invoked to explain the reaction are:

$$H^1(p,\beta^+\nu)H^2(p,\gamma)He^3 \begin{cases} (He^3,2p)He^4 & (1) \\ (\alpha,\gamma)Be^7 \begin{cases} (e^-\nu)Li^7(p,\alpha)He^4 & (2) \\ (p,\gamma)B^8(\beta^+\nu)Be^8(\alpha)He^4 & (3) \end{cases} \end{cases}$$

The energies released in the three possible chains, exclusive of neutrino energy losses, are different, being 26.2 Mev, 25.6 Mev and 19.1 Mev in reactions (1), (2) and (3) respectively. It is interesting to note that if the process proceeds by reaction (3) considerable energy escapes (29%) from the system via the very energetic neutrinos accompa nying the 15 Mev β^+ decay of B^8.

A factor affecting the relative importance of chains (2) and (3) is the relative probability that Be^7 will be destroyed by electron or by proton capture. The capture cross-section of the latter reaction, $Be^7(p,\gamma)B^8$, has not been reported as yet for protons, however.

The choice between chains (1) and (2) is greatly affected by the size of the capture cross-section of He^3 for α-particles in the reaction $He^3(\alpha,\gamma)Be^7$. No cross-section for this reaction was known until recently when Holmgress and Johnston (1959) measured it using a He^3 gas target. A check on this cross-section may also be made from the cross-section of the mirror reaction $T(\alpha,\gamma)Li^7$. Both Holmgren and Johnston (1959) and Riley (1958) have measured this value for α-particle energies from 0.47 to 2 Mev and while their results agreed within the combined uncertainties large errors were quoted amounting to at least 30% in each case. It was therefore felt that a more accurate determination of the absolute cross-section would be of some value. In order to give a good estimate of the absolute

cross-section and also to aid in understanding the nature of the reaction angular distribution measurements on the direct radiative capture gamma rays have been made. This latter investigation was also prompted by the anisotropy of 0.39 ± 0.37 observed by Riley at 1.6 Mev bombarding energy.

Chapter II

Experimental:

1. Apparatus

(a) Van de Graaff Generator

The source of the ion beam for the experiment to be described was the University of British Columbia's Van de Graaff electrostatic generator. Beams of singly ionized alpha particles of energies up to 2 Mev and of intensity on the target up to 10 microamperes were available. The straight down beam from the accelerating column was bent through 90^{o} by a large electromagnet into a horizontal glass sidearm tube with a target at the end. Careful alighment and focussing of the beam entering the top of the magnet was necessary to avoid having it strike the magnet box and cause a large increase in neutron induced background from reactions such as $C^{13}(\alpha,n)O^{16}$; the carbon arising because of the presence of diffusion pump oil vapor.

The long term stability of the magnetic field has been measured to be of the order of 3 parts in 10,000 by Aaronson (1950) and so was of negligible concern in this experiment. The energy of the accelerated particles was read on a generating voltmeter which looked at the high voltage dome. Any variation in alpha particle energy reaching the target as read by this voltmeter was less than 3 Kev. Calibration of the energy scale was carried out by observing the resonances of F^{19} under proton bombardment of 0.340, 0.8735 and 1.372 Mev. energy. The cali-

FIGURE 2 SIDEARM ARRANGEMENT

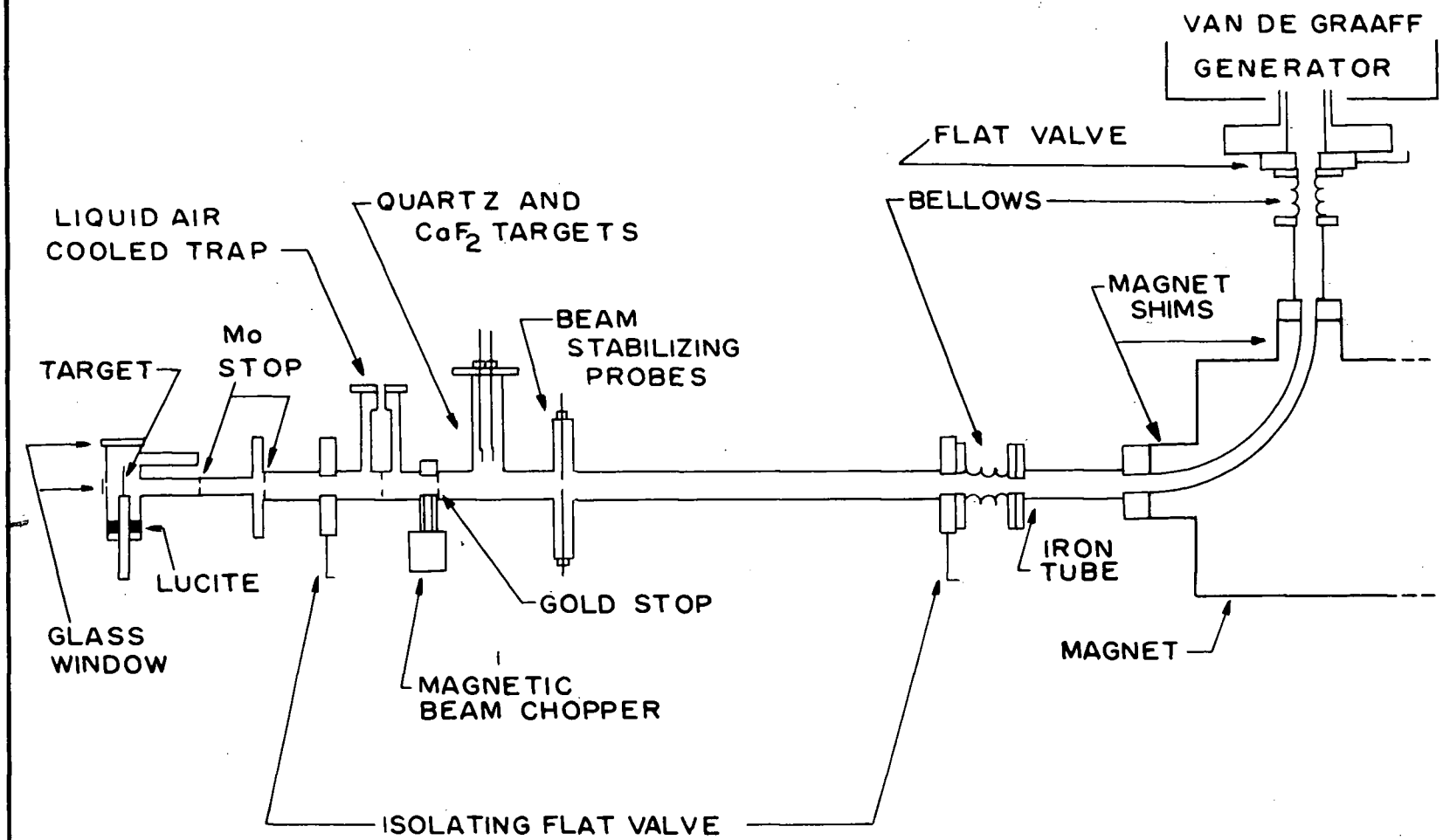

bration remained constant to $\pm$ 1.5 Kev over a period of 6 months.

(b) Sidearm Arrangement

The experimental arrangement of the target tube and the sidearm is shown in Figure 2. The total length of the horizontal sidearm was about 6 feet and it was located 44½ inches off the floor. Provision for lining the sidearm up optically before running a beam was made by having a small (1/16") glass window in the 1/16" brass target pot wall on the axis of the sidearm tube. A gold stop of 1 cm. diameter was used part way along the tube and two others of molybdenum (3/8"x 3/16") in the target pot itself in order to define the beam. These materials of high atomic number were used in order to reduce any Coulomb-excited background.

A liquid air cooled trap was mounted in front of the target chamber to condense out diffusion pump oil vapors present in the tube. Occasionally, the magnet box was cleaned with steel wool and hot dilute nitric acid to reduce background from straight down beam components other than those of mass 4. The target pot and molybdenum stops were cleaned before each run.

In order to measure the beam current the target holder was insulated from the target pot with a lucite spacer and 90 volt positive potential was applied to it to reduce secondary electron emission from the target. This target current was

measured on a current integrater (Edwards, 1950) on the 1.0 μf scale where one integrator count corresponded to about 106 microcoulombs with the exact value dependent upon the magnitude of the current being measured. This device was calibrated frequently and observed to stay constant to within 1%.

(c) Scintillation Counter

(i) Shielding

Two scintillation counters were tried for this experiment; one, consisting of a $2\frac{3}{4}$"x$4\frac{1}{2}$" NaI(Tl) crystal mounted on a Dumont K1213 photomultiplier tube and the other a $2\frac{1}{2}$"x$3\frac{1}{2}$" NaI(T4) crystal on a Dumont 6363 photomultiplier as used by Riley. Both counters gave good spectra for trial runs of alpha particles on a tritium target with heavy lead shielding. The beam dependent background counts, found by running the beam on a piece of zirconium, were in the ratio of the volumes of the two crystals. For the larger crystal this background in the 2 to 3 Mev region of the spectra amounted to 27 counts per minute per Mev at the 1.6 Mev bombarding energy. Because of a larger volume and noticeably better resolution the large crystal was the one chosen for use in this experiment.

For most of the $T(\alpha, \gamma)Li^7$ runs the end of the counter was placed about 6 cm. from the outside of the 2" diameter target pot. In all runs the counter and target pot were surrounded by about 5" of lead on all sides. In addition a lead wall was put up between the counter and the magnet box while wax was

FIGURE 3 SCINTILLATION COUNTER EFFICIENCY
(2¾" X4½" NaI Crystal)

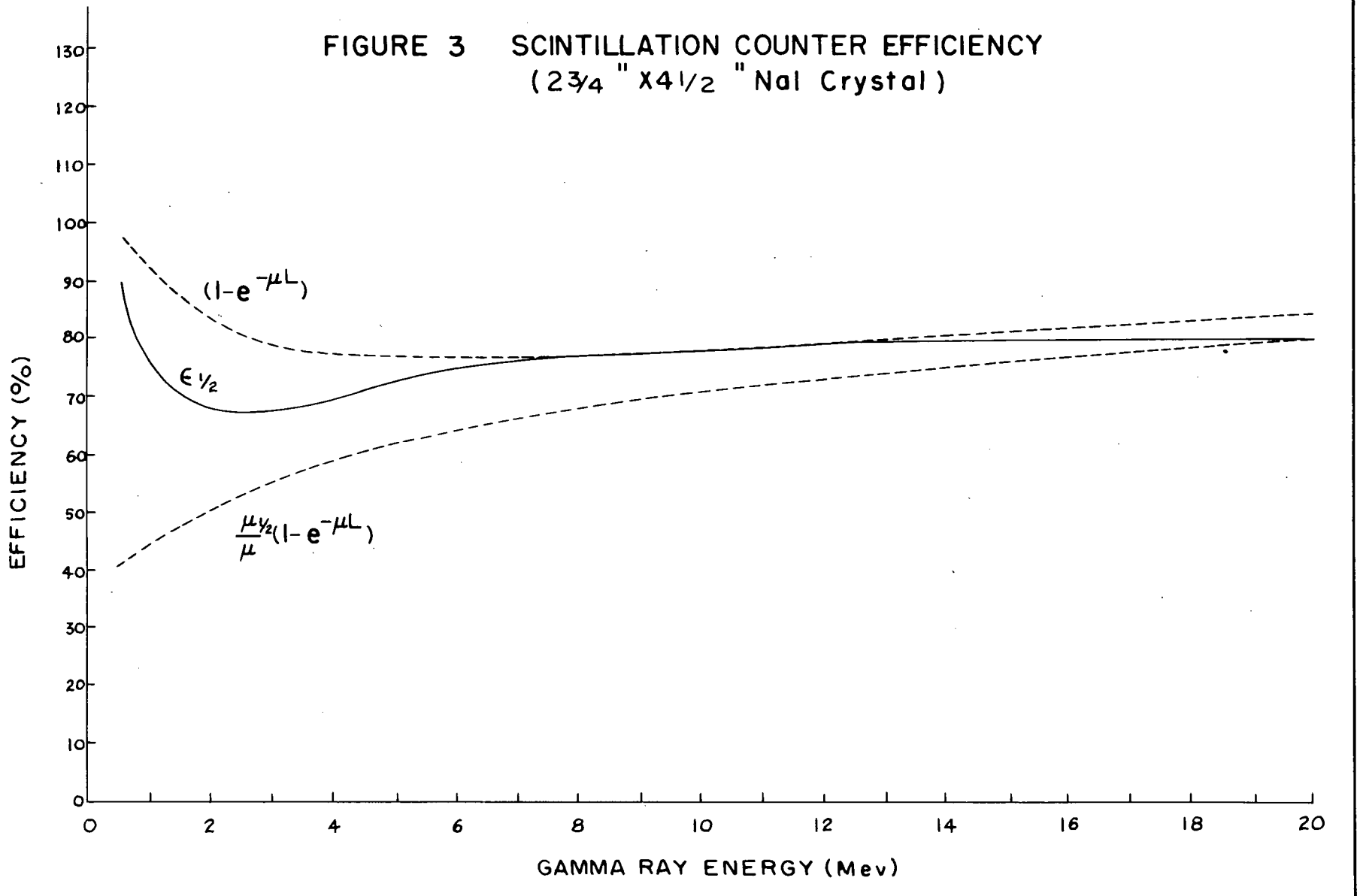

present between this wall and the magnet box. These materials shielded the counter from any (α,n) or (d,n) reactions of the beam with pump oil vapors in the magnet box.

(ii) Efficiency

In gamma ray flux measurements where scintillation counters are employed the counter efficiency must be found for the particular gamma ray energies involved. A commonly used value is that deduced from the total theoretical absorption coefficient, μ, for the particular crystal and gamma ray energy and defined as $(1-e^{-\mu L})$ where L is the length of the scintillating crystal. When using this efficiency, which is plotted as a function of energy for a particular NaI crystal in Figure 3, the total number of counts recorded by the counter are usually found from the gamma ray spectrum by extrapolating the spectrum to zero energy with a flat tail from the minimum which occurs at about half the full gamma ray energy. The correctness of this method is in doubt, however, for the following reason: in the B^{11} (p,γ)C^{12} spectrum, obtained at a low bombarding energy with a NaI crystal at 90° to the beam direction, the total number of 12 Mev counts is greater, by about 20 to 25%, than the total number of 4 Mev counts as determined by the above method. This contradicts the fact that the 4 Mev and the 12 Mev radiations have the same intensity in the 90° direction (Ajzenberg and Lauritsen, 1955). A variation in total absorption coefficient of NaI cannot account for this since it causes only

a 3% difference in the two efficiencies as defined above and as can be seen from Figure 3.

In an attempt to clear up such a serious inconsistency in flux measurements the efficiency has been defined in a slightly different manner in this laboratory. The proceedure is to define the efficiency to the half-energy bias as the ratio of the total counts above the half-energy point on the gamma ray spectrum to the total number of gamma rays incident on the crystal. Experimentally, efficiencies defined in this way have been measured at 0.51 Mev and 1.25 Mev using the radiations from calibrated sources of Na^{22} and Co^{60} respectively. A point at 6.14 Mev was also obtained from $F^{19}(p,\alpha,\gamma)O^{16}$ radiation, the absolute yield being determined from alpha particle counting as described in Part II of this thesis. Unfortunately no efficiency determination could be made at higher energies since the absolute yield of gamma rays from any possible reaction was not known with sufficient accuracy. However, an extrapolation was preformed as in Figure 3 to higher energies keeping the extrapolated curve between those for $(1-e^{-\mu L})$ and for $\frac{\mu_{\frac{1}{2}}}{\mu}(1-e^{-\mu L})$. The former is the total theoretical efficiency based on primary absorption processes only while the latter is the theoretical efficiency considering primary absorption processes which leave more than half the gamma ray energy in the crystal, that is, the contribution from the primary compton tail below half energy

has been dropped and the transfer of pulses above and below the half energy point due to secondary processes in the crystal has not been considered. This empirical curve for the efficiency as a function of energy is believed to be accurate to within 5%, up to 12 Mev and to within 10% from 12 to 20 Mev. Partial justification for the shape drawn is obtained from the results of the standard G-M counter efficiency determination to be described in Part II. The shape found for this efficiency versus energy curve was dependent upon the scintillation counter efficiency assumed and since a smooth curve was found the values used for the scintillation counter are believed to be correct to within the stated error.

Another characteristic of the scintillating crystal used was its effective centre distance. This distance from the crystal face to its effective centre may be found theoretically as $t = -\frac{\ln[0.5(1+e^{-\mu L})]}{\mu}$. However this is found to disagree with experimental determinations (Riley, 1958). Since these distances as a function of gamma ray energy have not been measured for the $2\frac{3}{4}$"x$4\frac{1}{2}$" crystal used, values were assumed on the basis of previous measurements on the $2\frac{1}{2}$"x$3\frac{1}{2}$" crystal. The uncertainty in such an estimate is believed to be less than $\pm$ 0.5 cm.

The experimental values of efficiencies described above are defined for the NaI crystal in a lead castle and the

FIGURE 4 BLOCK DIAGRAM OF ELECTRONICS

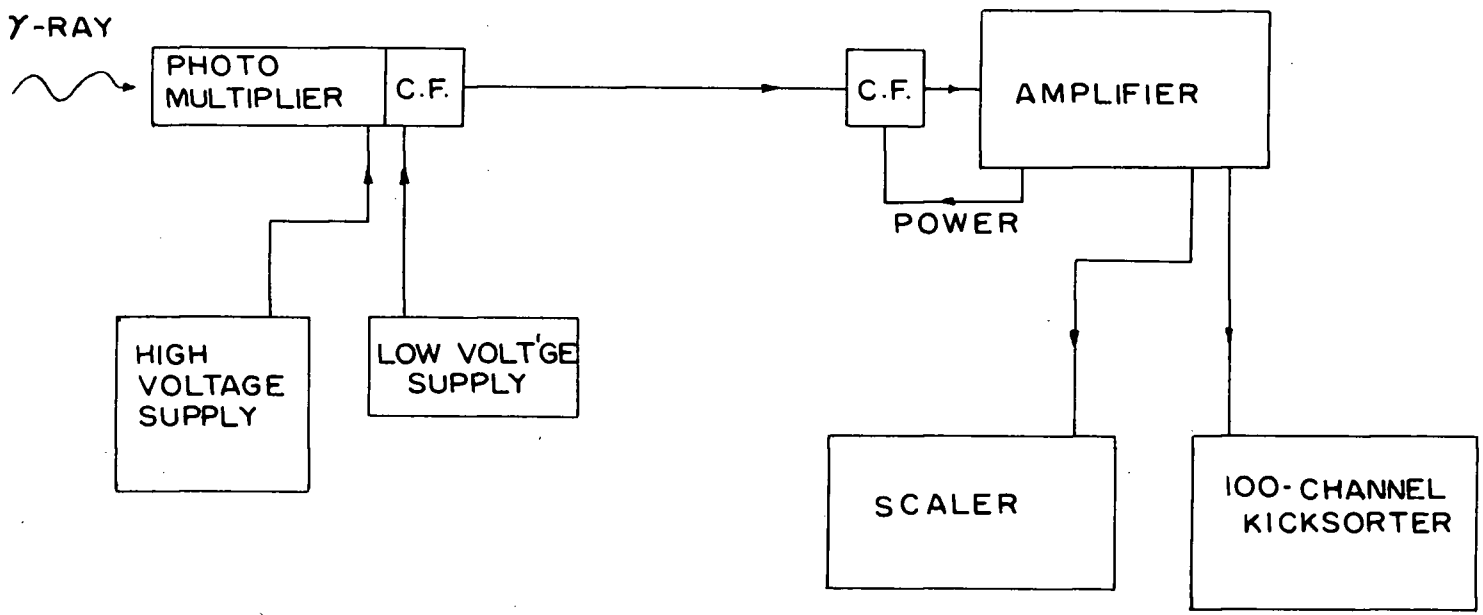

fact that more lead was used in the experiment than in the efficiency measurements makes a slight difference which was not allowed for. This, therefore, will introduce a small unknown error into absolute flux measurements.

(d) Electronics

High voltage for the photomultipliers was usually about 925 volts supplied by an Isotopes Development E.H.T. supply. Negative output pulses from a 403B cathode follower were fed into a long 100 ohm cable to another cathode follower unit used to drive a Dynatron Radio Limited amplifier Type 1430A. Positive pulses from this unit were fed to a Dynatron Radio Limited scalar Type 1009A in parallel with a 100-channel Computing Devices of Canada kicksorter. A block diagram is shown in Figure 4. The electronic equipment was calibrated for linearity by feeding pulses from a mercury relay pulse generator (Roberston, 1957) into the 403B cathode follower unit on the scintillation counter. The photomultiplier was calibrated separately by means of a RdTh source which also set the energy scale on the kicksorter.

2. Tritium Target

(a) Mounting

The tritium-zirconium target (#4) used in this experiment consisted of a small amount of tritium adsorbed in a thin evaporated film of zirconium on a platinum backing disc

of thickness 0.25 mm and diameter 1". The amount of zirconium present as specified by the suppliers, Oak Ridge National Laboratory, was 0.002705 gm on the 5.07 cm^2 disc area. The tritium content as measured by the above laboratory was 731 millicuries on April 30, 1959.

In order to prevent loss of tritium caused by target heating when a beam was being run precautions were taken in the mounting arrangement. The thin target disc was held rigidly against a thick (1/32") copper backing plate which was in turn clamped to a copper supporting rod. Thus, good heat conduction away from the target was obtained. In addition the lower end of the supporting rod was cooled with forced air. A piece of lucite with angle markings on it was placed over the glass window on the top of the target pot to enable any target angle to be set easily.

(b) Tritium Content

The amount of tritium on the target was estimated in two ways:

(i) β-Activity

Allowing for the decay of 1% of the tritium with a characteristic half-life of 12.26 years from the time of the Oak Ridge National Laboratory's activity measurement to the time the experiment was carried out, the tritium content estimated from the β-activity was 15.0×10^{18} atoms of tritium, or 2.95×10^{18} tritium atoms per cm^2. Since the amount of zirconium

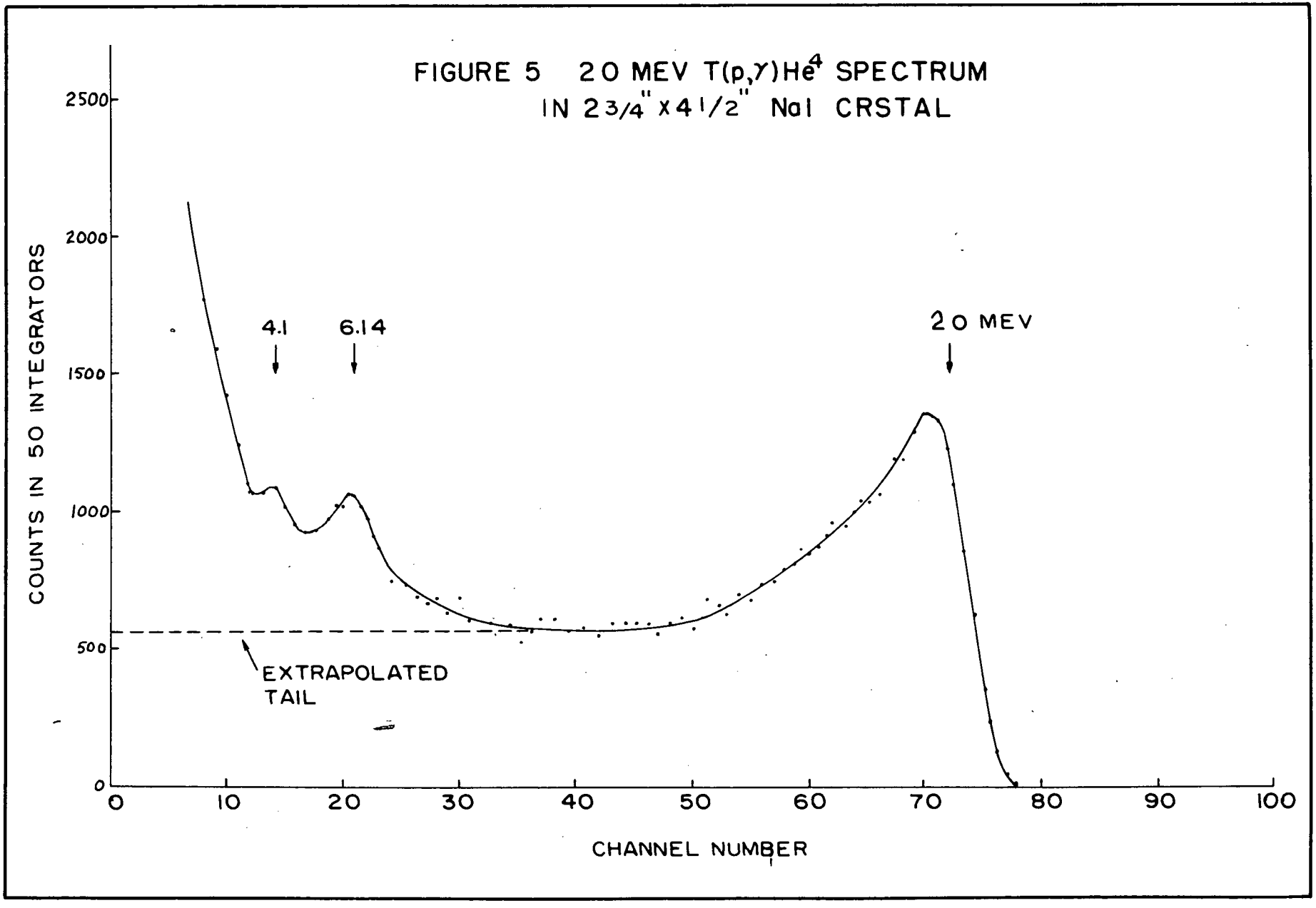
FIGURE 5 20 MEV T(p,γ)He4 SPECTRUM
IN 2 3/4" X 4 1/2" NaI CRSTAL
COUNTS IN 50 INTEGRATORS
2500
2000
1500
1000
500
0
4.1
6.14
20 MEV
EXTRAPOLATED
TAIL
0
10
20
30
40
50
60
70
80
90
100
CHANNEL NUMBER

present was 3.53×10^{18} atoms per cm^2 of target area the tritium to zirconium atomic ratio may be found as 0.84:1.

(ii) $T(p,\gamma)He^4$ Yield

Towards the end of the $T(\alpha,\gamma)Li^7$ work it was decided to measure the tritium target content by means of the $T(p,\gamma)He^4$ yield using the 90^o differential cross-section data of Perry and Bame (1955). Accordingly, two $T(p,\gamma)He^4$ runs were taken separated and preceeded by runs of $T(\alpha,\gamma)Li^7$ with the counter at 90^o to the beam. All of these runs were done on the same spot on the target, with the same heavily shielded scintillation counter and the same counter-to-target distance. For the $T(p,\gamma)He^4$ reaction the 20 Mev spectrum in Figure 5 was observed with the 100-channel kicksorter at bias 1.

The scintillation counter efficiency used for this 20 Mev radiation was not that defined to the half energy bias but the one defined as $(1-e^{-\mu L})$ the total number of recorded events being found by extrapolating the smooth tail of the 20 Mev spectrum to zero pulse height as shown in the figure. This doubtful method was applied since it was the same one used by Perry and Bame in establishing their cross-section, so that if any error is introduced by the method it should be cancelled in finding the target tritium content.

To record the spectrum shown a beam of about 7 microamperes of protons at 800 kev energy was used. This energy was chosen for two reasons: first, to be below the $T(p,n)He^3$ threshold

FIGURE 6 GAMMA RAY ABSORPTION FACTOR FOR TARGET BACKING

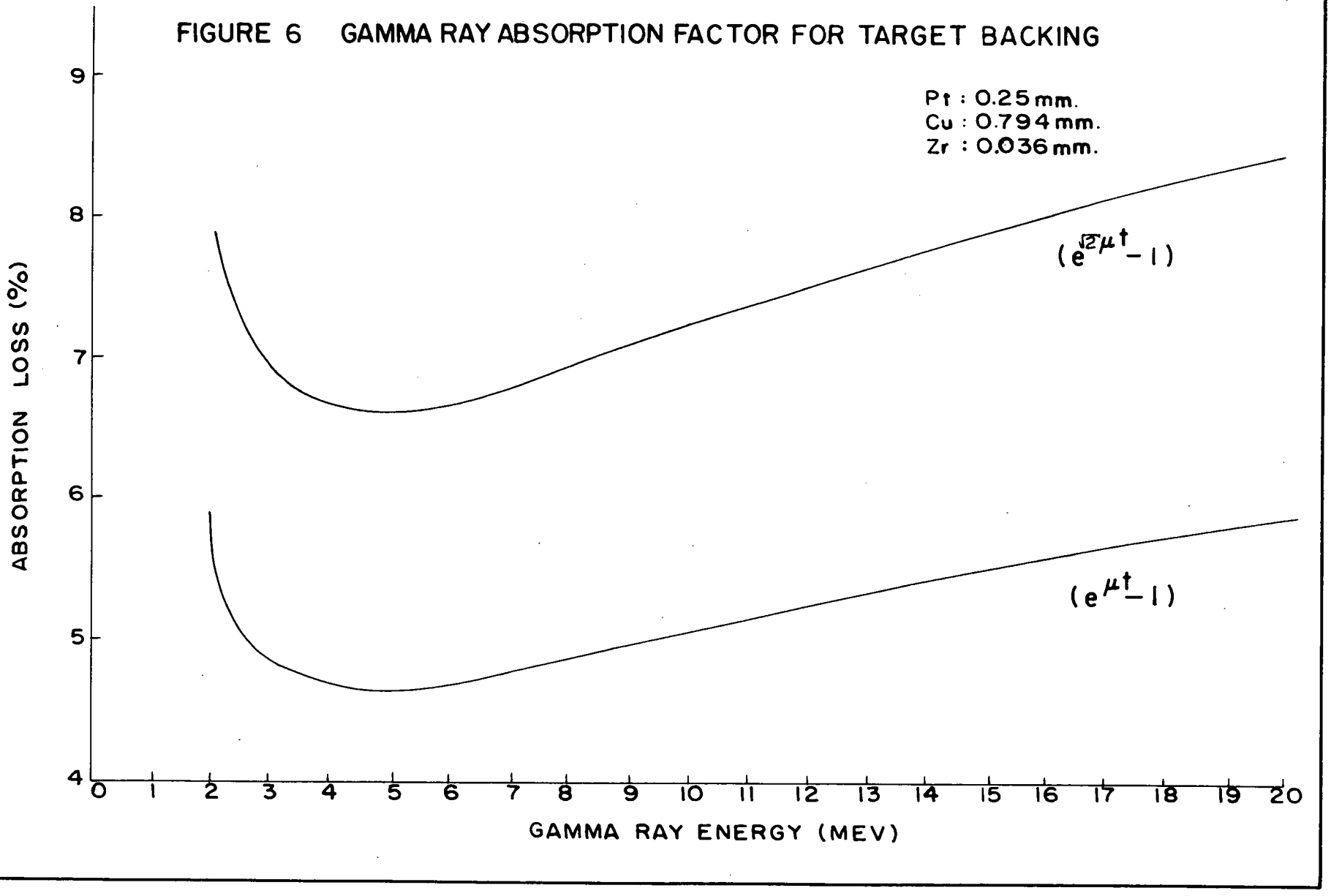

at 1.0 Mev and, second, to avoid the 0.873 Mev resonance of F^{19} as much as possible since fluorine was known to be on the target. Even at 800 kev, however, some $F^{19}(p,\alpha,\gamma)O^{16}$ 6.14 Mev gamma rays were observed. The spectrum shown has been corrected for beam dependent background found by reversing the target and running the beam on a thin (.0014") zirconium strip on the back for the same length of time and number of integrator counts as in a $T(p,\gamma)He^4$ run. This background was so small that it would not show up in the figure above about channel 30.

During the runs the front face of the scintillation counter was 5.96 cm away from the outside of the brass target pot and the target was positioned at 45^o so that the reaction gamma rays passed through the target backing. For an effective centre distance, from the front face of the crystal, estimated to be 4.0 cm. a spacing of 1.034 cm between the crystal and the aluminum can covering the crystal, and a target pot radius of 2.54 cm. the solid angle subtended by the crystal, for 20 Mev gamma rays, at the target was found to be 0.198 steradian.

The absorption correction for loss of gamma ray intensity in the target backing of platinum-copper-zirconium may be read from the curve in Figure 6. Applying also a correction for gamma ray absorption in the 1/16" target pot walls results in a final factor of 1.137.

FIGURE 7 STOPPING CROSS SECTION, ϵ, IN Zr-T

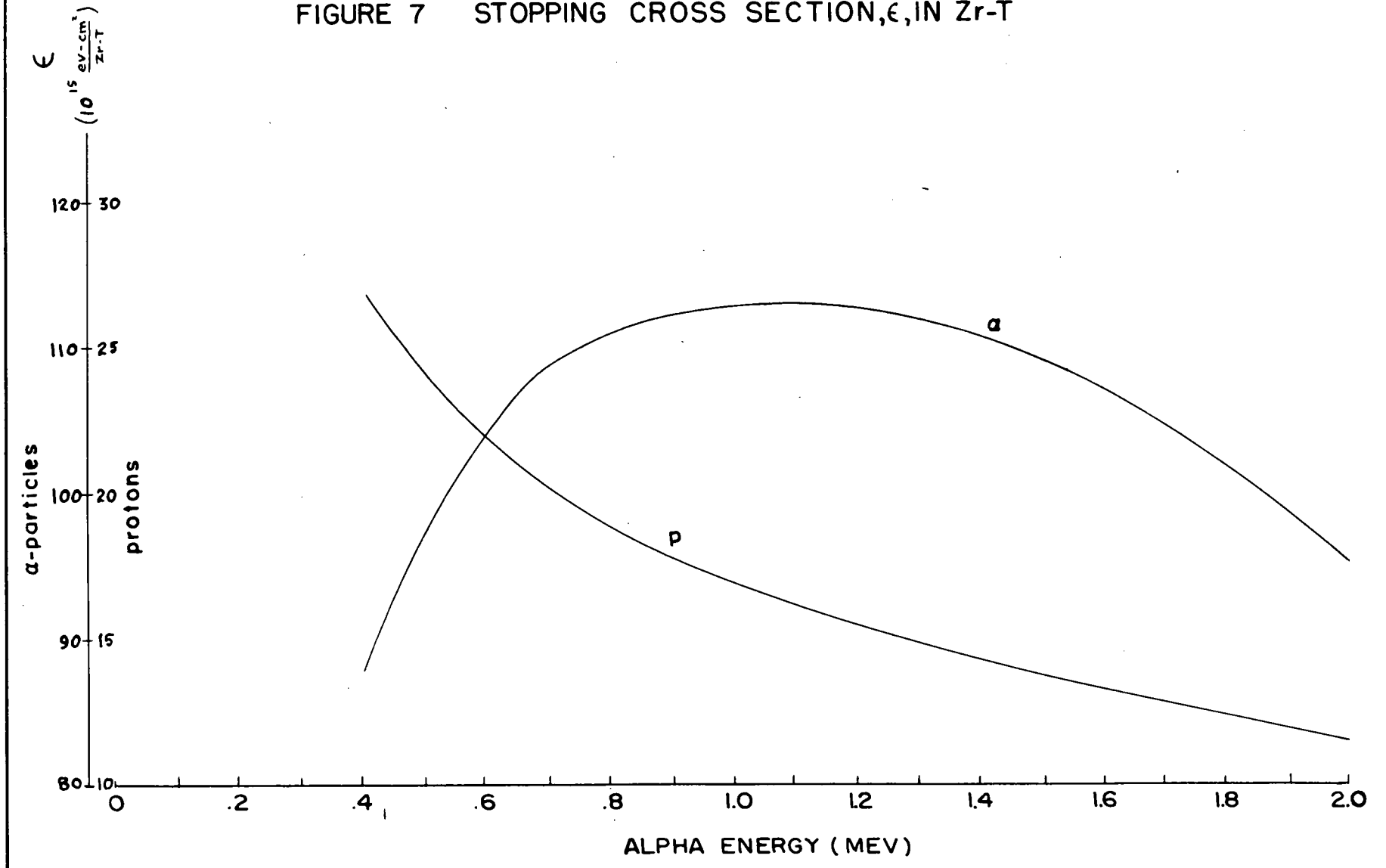

Hence, the number of tritium atoms on the target may be calculated from the following data:

$Nc = 62920 \pm 7\%$

$= 64120 \pm 7\%$ after correcting for the effect of the counter solid angle on the $\sin^2$ angular distribution of 20 Mev gamma rays.

$\Omega = 0.198 \pm 6\%$

$\epsilon = 1-e^{-L} = 0.837 \pm 10\%$

$$Np = \frac{(50 \text{ integrator counts})(103.8\times10^{6})}{1.6\times10^{-19}} = 3.24\times10^{16}$$

protons $\pm$ 1%

$$\left(\frac{d\sigma}{d\omega}\right)_{90^\circ} = 2.666\times10^{-30}\text{cm}^2/\text{steradian} \pm 10\% \text{ for } \bar{E}p = 753 \text{ kev.}$$

The target thickness for 800 kev protons was found from the curve in Figure 7, drawn from Whaling's (1958) data, as 95 kev $\pm$ 5% for the target at 45°. Hence the mean proton energy in the target was found to be $\bar{E}p = 800-\frac{95}{2} = 753$ kev and the above 90° differential cross-section value was obtained for this energy from Perry and Bame (1955)

$$\therefore \quad n_T = \frac{Nc}{Np\left(\frac{d\sigma}{d\omega}\right)_{90^\circ}\cdot\Omega\cdot\epsilon} = 4.48\times10^{18} \text{ atoms/cm}^2 \pm 18\%$$

for the atomic surface density of tritium.

This, then, leads to a tritium-zirconium ratio of 1.3:1 which is in quite violent disagreement with the β activity

measurements which gave 0.84:1. This might be explained by a very non-uniform distribution of the tritium on the target surface. It is interesting to note that the supplier, Oak Ridge National Laboratory, claims that the tritium-zirconium rates on their targets is always at least 1:1 and may be as high as 1.8:1. Since their β activity measurements contradict this on a number of tritium targets received from them their activity measurements may be at fault; possibly all the low energy beta rays do not escape from the thin zirconium layers used for these targets.

(c) Target Thickness for Alpha Particles

Since the stopping cross-section of tritium atoms is small compared to that for zirconium atoms a 1:1 ratio of tritium to zirconium was assumed in order to make use of the curves, shown in Figure 7, deduced from Whaling's report, to find the stopping cross-section for alpha particles.

Suppose a particle of energy E_i is incident on a target of atomic surface density n (atoms per unit area) and emerges with an energy E_o. The loss in energy of the particle may be written $\Delta E = E_i - E_o = \int_o^n \frac{(dE)}{(dx)} \cdot \frac{dn}{N} = \int_o^n \epsilon \, dn$ where N is the atomic density of the target material (atoms per unit volume) and ϵ is the stopping cross-section that Whaling tabulates as a function of energy. From this formula, knowing the atomic surface density, the target thickness in electron-volts may be found. However, the numerical integration is

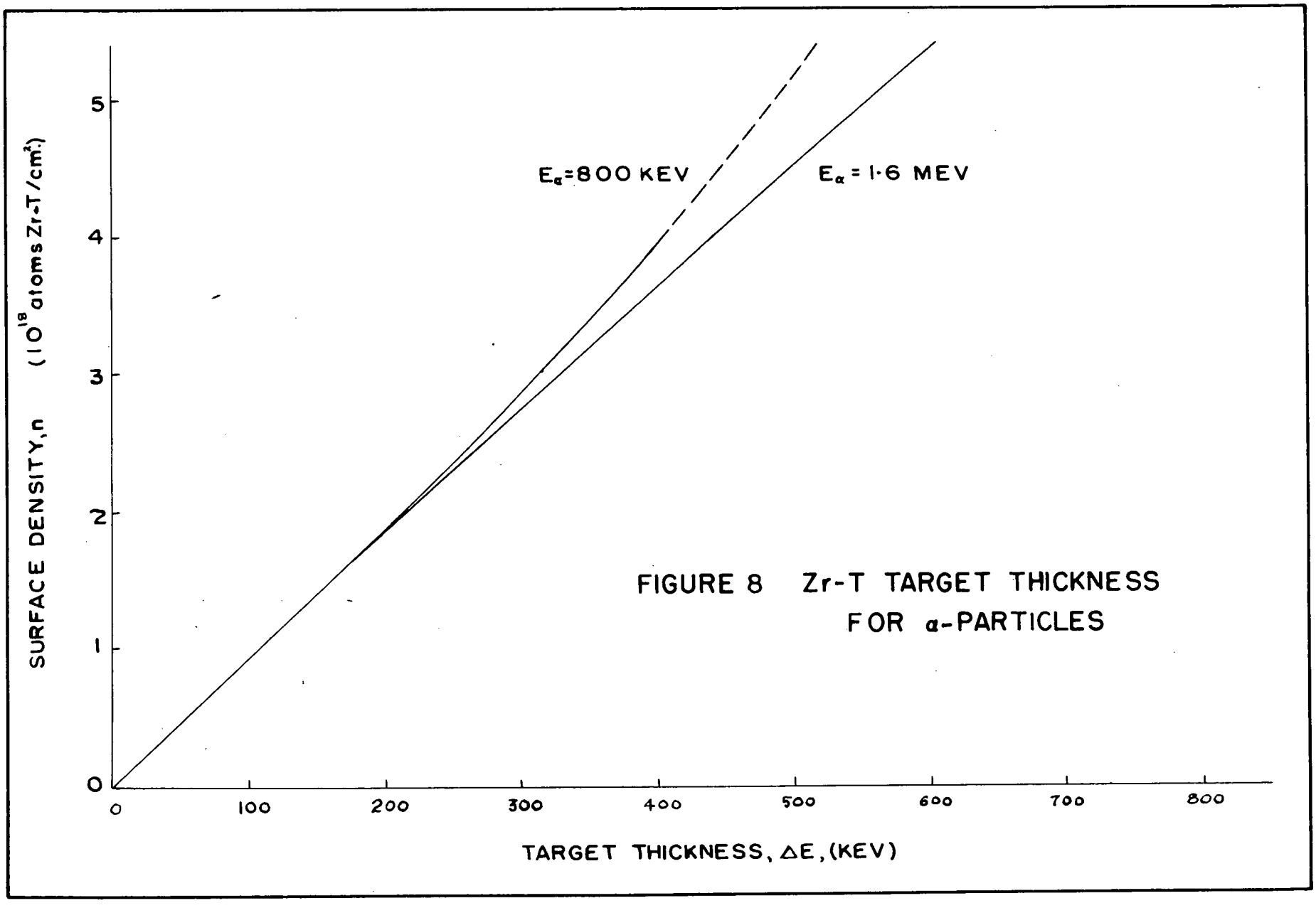

FIGURE 8 Zr-T TARGET THICKNESS FOR α-PARTICLES

rather tedious and so a single transformation may be made to another form where $n = \int_{E_o}^{E_i} \frac{dE}{\epsilon}$. In this form n may be given easily in terms of E_o for a fixed E_i, the proceedure being to plot $1/\epsilon$ as a function of energy and doing a single numerical integration. Such a plot for E_i equal to 1.6 Mev and 800 kev is given in Figure 8.

For the target used in this experiment the surface density of zirconium-tritium pairs was taken to be $n_{Zr-T} = 3.53 \times 10^{18}$ Zr-T atoms/cm^2 based on the Oak Ridge measurement of the surface density of zirconium on the target. For the target operated at 45° to the beam this value was increased to 5.00×10^{18} Zr-T atoms/cm^2. Using Figure 8 the following may be calculated:

E_α	Target Angle	n_{Zr-T}	ΔE	$\overline{E}_\alpha = E_\alpha - \frac{\Delta E}{2}$
(Kev)	(degrees)	Zr-T atoms /cm^2	(Kev)	(Kev)
800	90	3.53×10^{18}	364	618
	45	5.00	480	560
1600	90	3.53	394	1400
	45	5.00	560	1320

3. Angular Distribution Measurements

(a) Procedure

The main energy chosen for the angular distribution measurement was 1.6 Mev since a good yield was obtained and since

Riley's normalization occured at this energy. In these runs the $2\frac{3}{4}$"x$4\frac{1}{2}$" NaI (Harshaw) crystal was used and the scintillation counter positioned by means of a lucite spacer so that its front face was 5.96 cm from the outside of the target pot.

Since it was known from Riley's runs and the low cross-section obtained that background counts could be troublesome care was taken to reduce these to a minimum as described in Section 1 (c) (i). At the 1.6 Mev bombarding energy a target current of 3 to 4 microamperes was maintained for 50 integrator counts in about 25 minutes. This target current measurement was used as the monitor and target deterioration checked by repeat runs at the 90° counter position. No sign of target loss was noticed at any time.

Runs were taken with the counter at 0°, 45°, 90° and 134° to the beam direction on each side of the beam. At certain counter angles the target was set at 90° to the beam and at other angles it was set at 45° to the beam in order to avoid excessive absorption of gamma rays in the target backing. A proceedure which eliminated any effect of right-left asymmetry was to run at counter angles 0° and 90° (both sides of the beam) with the target at 45°, turn the target through 90° and repeat the measurements at the same counter angles.

For all runs taken spectra were recorded showing transitions in Li^7 to the ground state, γ_1, to the first excited state

γ_2 and from the first excited state to the ground state, γ_3.

Measurements were also made at an 800 kev -particle bombarding energy. This energy was chosen because the yield was still quite high in order to see whether the angular distribution changed with bombarding energy. For this energy the counter was moved closer to the target pot, using a 2.12 cm. lucite spacer, since only the 0° and 90° angles were under investigation. A current of over 5 microamperes was run for 70 integrator counts taking about 25 minutes. Runs were taken with the target at 45° (both angles) only.

RdTh spectra were obtained frequently for energy calibration of the system. Occasionally, gain shifts of about 1 or 2 channels were observed probably due to a high counting rate in the scintillation counter so that all runs had to be corrected for this before analyzing.

In spite of the liquid air trap before the target pot carbon was deposited on the target changing its color from a golden tan to a smudged brown appearance after a 1.6 Mev run and to light grey with blue edges after a run at 800 Kev.

The target was moved as little as possible in order to reduce the uncertainty in duplicating its angle and beam dependent background runs were then taken at the end of the work by reversing the target and running the beam on the piece

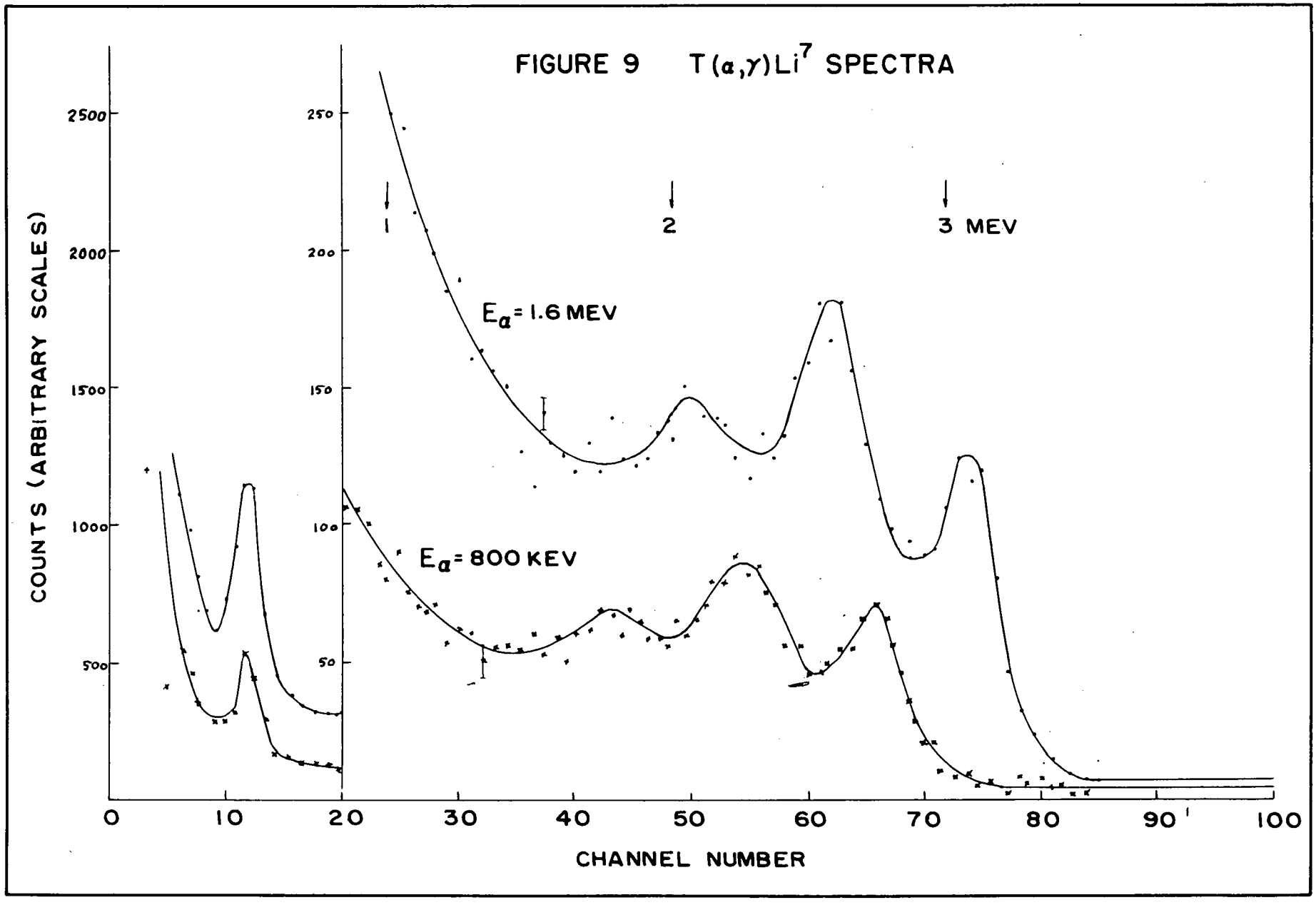
FIGURE 9 T(α,γ)Li7 SPECTRA
COUNTS (ARBITRARY SCALES)
2500
2000
1500
1000
500
250
200
150
100
50
1
2
3 MEV
Eα = 1.6 MEV
Eα = 800 KEV
0
10
20
30
40
50
60
70
80
90
100
CHANNEL NUMBER

of zirconium for the same number of integrator counts as during a regular run. The time dependent background was about $7\frac{1}{2}$ counts per minute per Mev in the region of gamma ray energies 2 to 3 Mev. The beam dependent background however went from 22 counts per minute per Mev at 1.6 Mev bombarding energy to 9 counts per minute per Mev at 800 Kev in the same region.

(b) Standard Gamma Ray Spectrum

After correcting for beam dependent background the $T(\alpha,\gamma)Li^7$ gamma ray spectra were plotted; typical spectra obtained at 1.6 and 0.8 Mev are shown in Figure 9. In addition to the $T(\alpha,\gamma)Li^7$ gamma rays it was apparent that there was some background present from the target itself similar to that observed by Riley. Because of this unknown amount of target dependent background two proceedures were possible for the analysis of the data. One was to make a rough estimate of this background by assuming that it decreased smoothly in the region of the 3 Mev gamma ray peaks down to the level of the tail extending beyond the peaks; upon subtraction the resultant spectrum was to be separable into two curves having standard shapes for gamma rays to the ground state and first excited state of Li^7. The alternative was to make a decomposition of the $T(\alpha,\gamma)Li^7$ gamma ray spectrum into its two gamma ray components of standard shape which could be subtracted leaving the target dependent background. Both methods were used, however the second one was considered more accurate.

FIGURE 10 STANDARD GAMMA RAY SPECTRUM

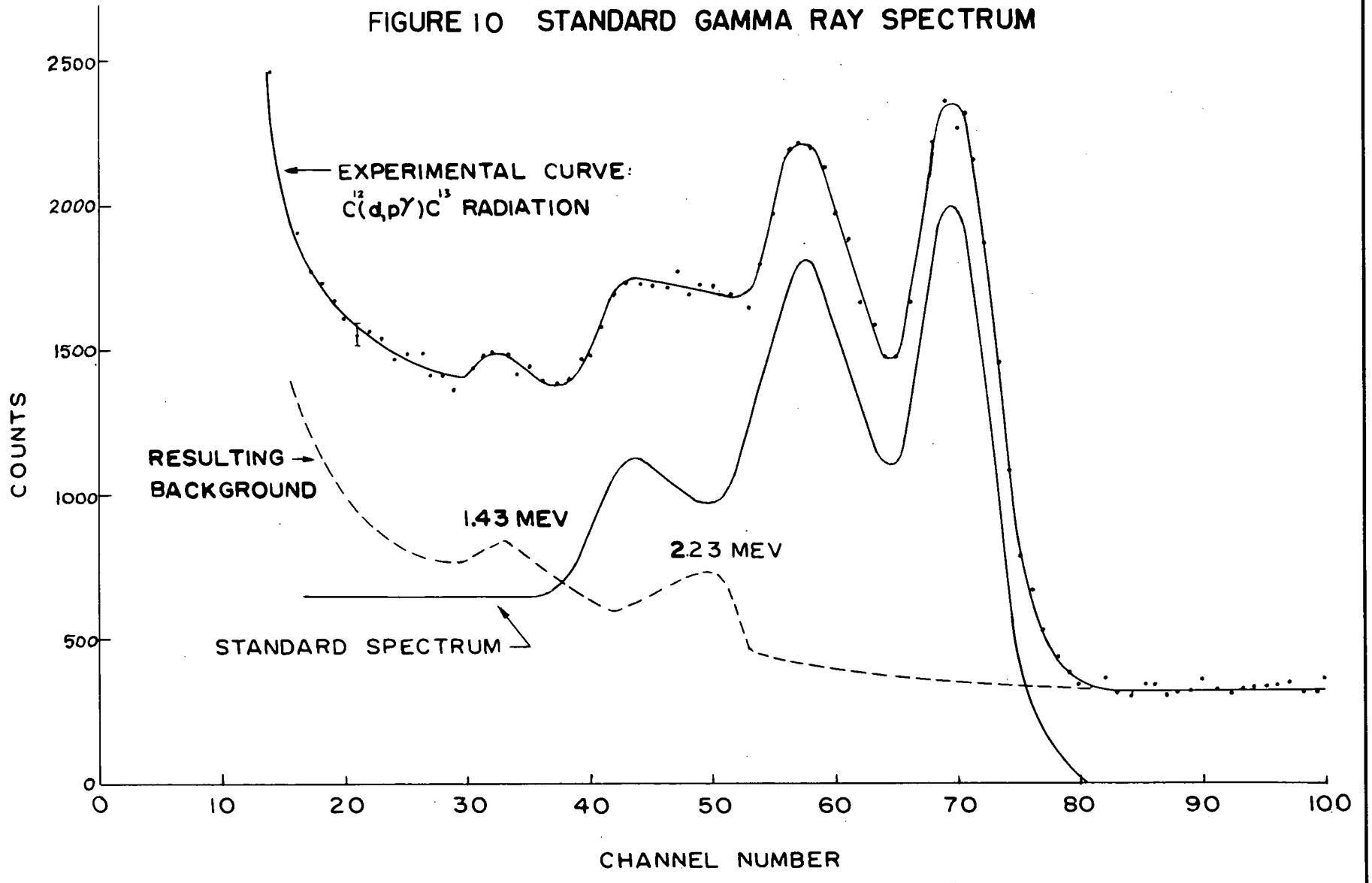

In order to make this analysis a 3 Mev spectrum of standard shape was obtained from comparisons of gamma ray spectra of 3.09 Mev from $C^{12}(d,p,\gamma)C^{13}$, 2.62 Mev from RdTh, 4.43 Mev from $B^{11}(p,\gamma)C^{12}$ and 6.14 Mev from $F^{19}(p,\alpha,\gamma)O^{16}$. The 3.09 Mev gamma ray from $C^{12}(d,p,\gamma)C^{13}$ would have been satisfactory as a standard by itself except for the neutrons from the $C^{13}(d,n)N^{14}$ reaction with the 1% of C^{13} in the natural carbon (Aquadag) target. The standard 3 Mev gamma ray spectrum is shown in Figure 10 as is the observed spectrum from $C^{12}(d,p\ )C^{13}$. The difference of the two gives a target dependent background showing peaks at 2.23 Mev from the reaction $H(n,\gamma)H^2$ of neutrons in wax near the counter and at 1.43 Mev resulting from a gamma ray in the decay of K^{40} in the NaI crystal.

(c) $\underline{T(\alpha,\gamma)Li^7}$ Spectra

About one half of the $T(\alpha,\gamma)Li^7$ gamma spectra taken were subjected to a decomposition into two standard gamma rays and a smooth background. The procedure was to fit the photopeak of the standard gamma ray spectrum to the upper peak in the $T(\alpha,\gamma)Li^7$ spectrum such that the difference, considered as background, joined continuously to the tail above the upper peak. The rest of the standard gamma ray spectrum was then constructed and subtracted from the $T(\alpha,\gamma)Li^7$ spectrum. A similar analysis was performed on the resulting curve using, as the standard gamma spectrum for γ_2, a good RdTh spectrum. The resulting background, however, had oscillations in it--the peaks

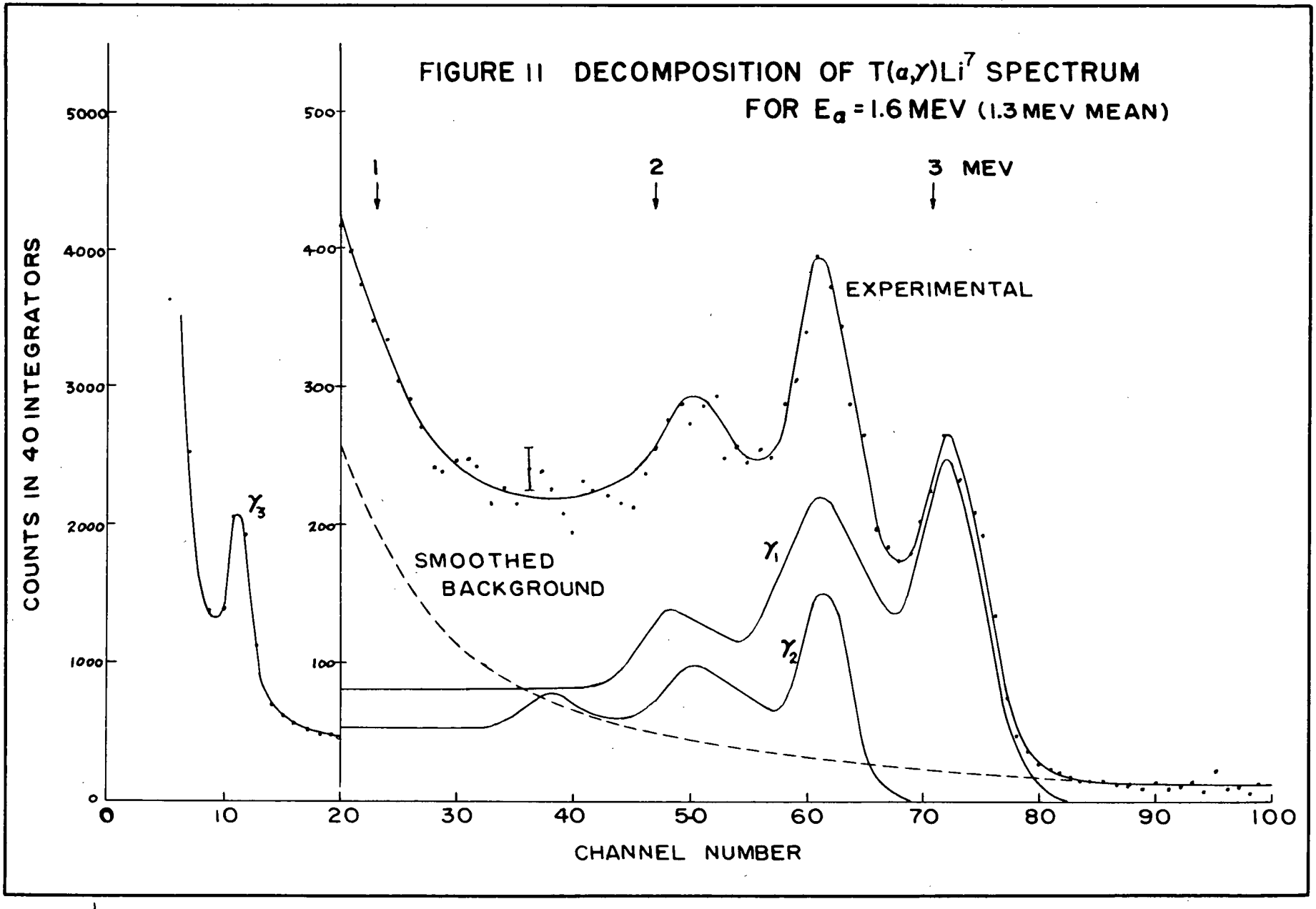
FIGURE 11 DECOMPOSITION OF T(a,γ)Li7 SPECTRUM
FOR Ea = 1.6 MEV (1.3 MEV MEAN)
1
2
3 MEV
EXPERIMENTAL
SMOOTHED
BACKGROUND
γ1
γ2
γ3
COUNTS IN 40 INTEGRATORS
CHANNEL NUMBER
5000
4000
3000
2000
1000
0
500
400
300
200
100
0
10
20
30
40
50
60
70
80
90
100

and valleys being observed to change position with changing particle energy. The reasons for this were two: first, because of statistical errors in the experimental curve and, second, because the peaks of the experimental curve were substantially broader than those due to monochromatic gamma rays on account of the thickness of the tritium target. No allowance for this latter effect had been made in constructing the standard gamma ray spectrum. Since a smooth background did not show up the two standard spectra corresponding to those for γ_1 and γ_2 were adjusted until the oscillations became a minimum and could be averaged to a smooth curve. The decomposition was then regarded as being accurate to almost within statistical errors. Such a break-up of a $T(\alpha, \gamma)Li^7$ gamma ray spectra for a bombarding energy of 1.6 Mev is shown in Figure 11.

After a number of curves had been analyzed in the above manner the general shape of the target dependent background became known and the remaining curves were subjected to analysis by the first method described above in 3(b).

$T(\alpha, \gamma)Li^7$ gamma ray spectra, corrected for a smooth background, taken at a bombarding energy of 1.6 Mev are shown in Figure 12 for the scintillation counter at 0° and 90°. It is clearly seen that the angular distribution of γ_1 and γ_2 is not isotropic. Also noticeable is the Doppler shift of the ground state transition gamma ray, γ_1.

FIGURE 12 $T(\alpha,\gamma)Li^7$ SPECTRA : ANGULAR DISTRIBUTION AT $\bar{E}_\alpha$ = 1.32 MEV

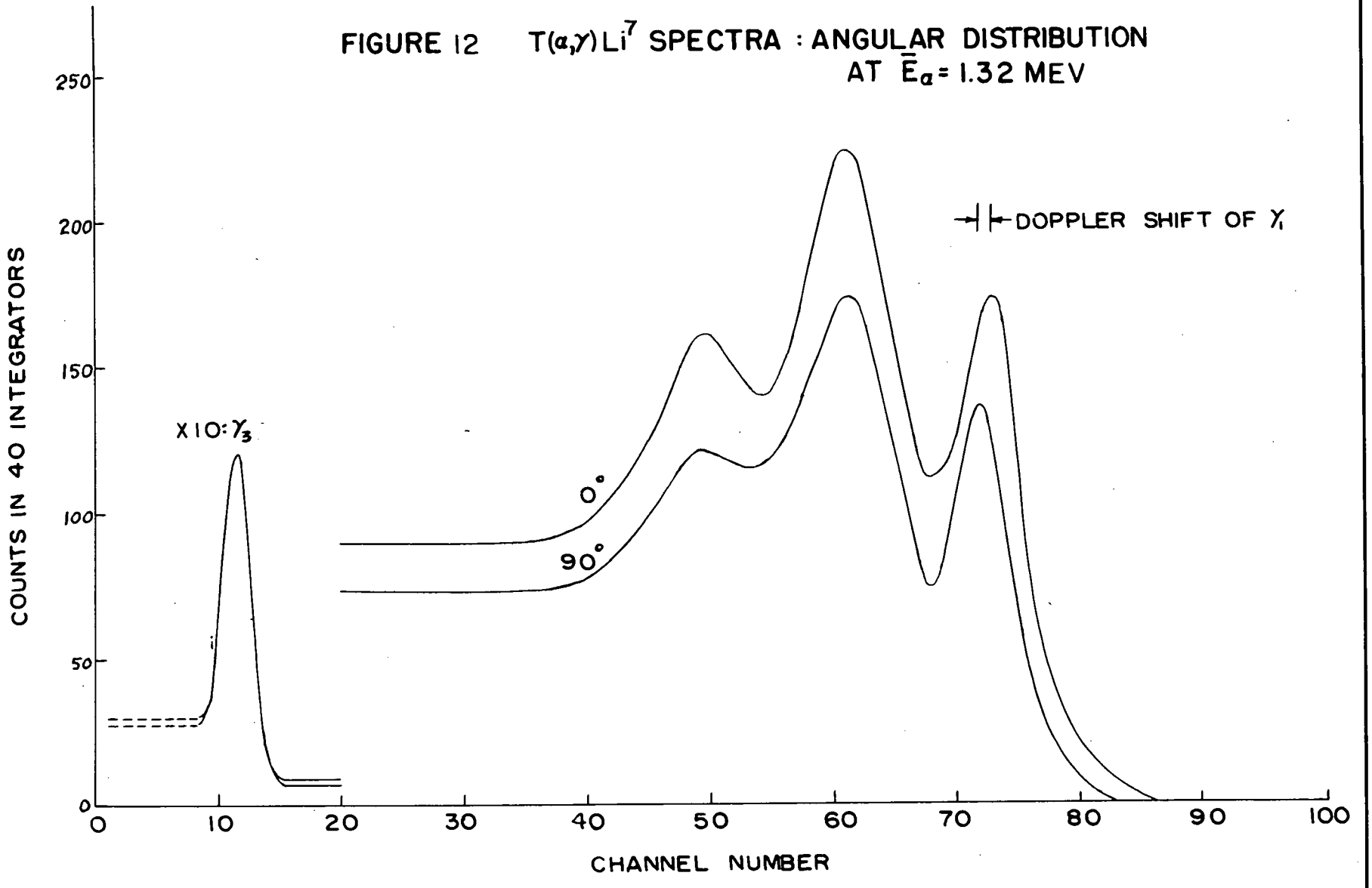

(d) Branching Ratio

As a consequence of the analysis used a branching ratio for the decay of Li^{7*} to the first excited state and ground state could be made. The scintillation counter efficiency defined to the half-energy bias was the same for both γ_1 and γ_2. Therefore the ratio of intensities of γ_1 to γ_2 was the same as the ratio of the number of counts above the half-energy bias in the γ_2 spectrum to the corresponding number in the γ_1 spectrum except for an absorption correction, which amounted to less than 1% for the ratio. Within the experimental accuracy the ratio was independent of angle indicating that γ_1 and γ_2 have the same angular distribution. Discrimination for the ratio at different energies could be made, however, with the results.

$$\frac{N_{\gamma_2}}{N_{\gamma_1}} = 0.446 \pm 0.014 \text{ at } E_\alpha = 1.6 \text{ Mev}$$

$$= 0.361 \pm 0.001 \text{ at } E_\alpha = 800 \text{ Kev}$$

$$= 0.524 \pm 0.08 \text{ at } E_\alpha = 500 \text{ Kev}$$

This last figure was based on a single run to be mentioned later. From the above figures the fraction of the total transition in Li^{7*} due to ground state, γ_1, decay may be found which are necessary for determining the cross-section.

$$\frac{N_{\gamma_1}}{N_{\gamma_1} + N_{\gamma_2}} = 0.69 \pm 0.007 \text{ at } E_\alpha = 1.6 \text{ Mev}$$

$$= 0.73 \pm 0.006 \text{ at } E_\alpha = 800 \text{ Kev}$$

$$= 0.66 \pm 0.04 \text{ at } E_\alpha = 500 \text{ Kev.}$$

(e) Angular Distributions

The simplest theoretical model for the $T(\alpha, \gamma)Li^7$ reaction is one in which it is assumed that the capture takes place with zero relative orbital angular momentum (S wave Alpha particles) from the continuum directly to the 3/2 ground state or the 1/2 first excited state with the emission of electric dipole radiation. On the basis of this model the angular distribution expected for the radiation can only be isotropic. However the preliminary measurements of P Riley (1958) at a bombarding energy of 1.6 Mev indicate that the ratio of the yield at 0° to that at 90° is 1.40 ± 0.37. In view of the interest in the reaction and the discrepancy of this result from the expectations of the simple model it was felt that the accuracy of the angular distribution data should be improved and extended to cover a wider range of bombarding energies.

Since the branching ratio for the two transitions γ_1, and γ_2 was independent of angle to within 3 percent indicating that the transitions to the first excited state and to the ground state had the same angular distribution, only the angular distribution of the ground state, γ_1 was analyzed in detail. The number of counts to the half energy bias in the γ_1 portion of the spectra at 0°, 45°, 90° and 135° on each side of the target were corrected for absorption losses and the values from at least 6 different runs averaged for each angle to give the

following results:

(i) 1.6 Mev - Mean alpha energy in the target = 1.32 Mev.

$$\frac{N0^{\circ}}{N90^{\circ}} = 1.30 \pm .04 \quad \frac{N45^{\circ}}{N90^{\circ}} = 1.08 \pm .06 \quad \frac{N134^{\circ}}{N90^{\circ}} = 1.04 \pm .06$$

The errors given above are based on the counting statistics but also are of the same order as the root mean square errors of the individual runs from the mean for each angle. The results show that the distribution is symmetrical about 0°, indicating that the line of the beam passed through the centre of the circle on which the counter rotated, and that it is to a good approximation symmetrical about 90° which suggests that there are no contributions from opposite parity incoming waves. Therefore the distributions should be fitted by an expansion in even powers of cosine θ only. If only dipole terms are included the expansion is then of the form $1+a\cos^2\theta$ and the 0° to 90° ratio requires a value of "a" of 0.30. This however gives a poor fit to the 45° and 135° values. Including, then, the next term in the expansion $1+a\cos^2\theta + b\cos^4\theta$ a good fit can be obtained with a = -0.06 and b = 0.36. It should be noted that the number of experimental points is not great enough to consider the inclusion of any high terms. These results were then corrected for the solid angle of the counter which increased the 0° to 90° ratio by 1.6% without significant effect on the other ratios. Next the ratios were transferred to centre of mass coordinates by use of the equations

FIGURE 13 ANGULAR DISTRIBUTIONS AT 1.6 MEV
(1.32 MEV MEAN)

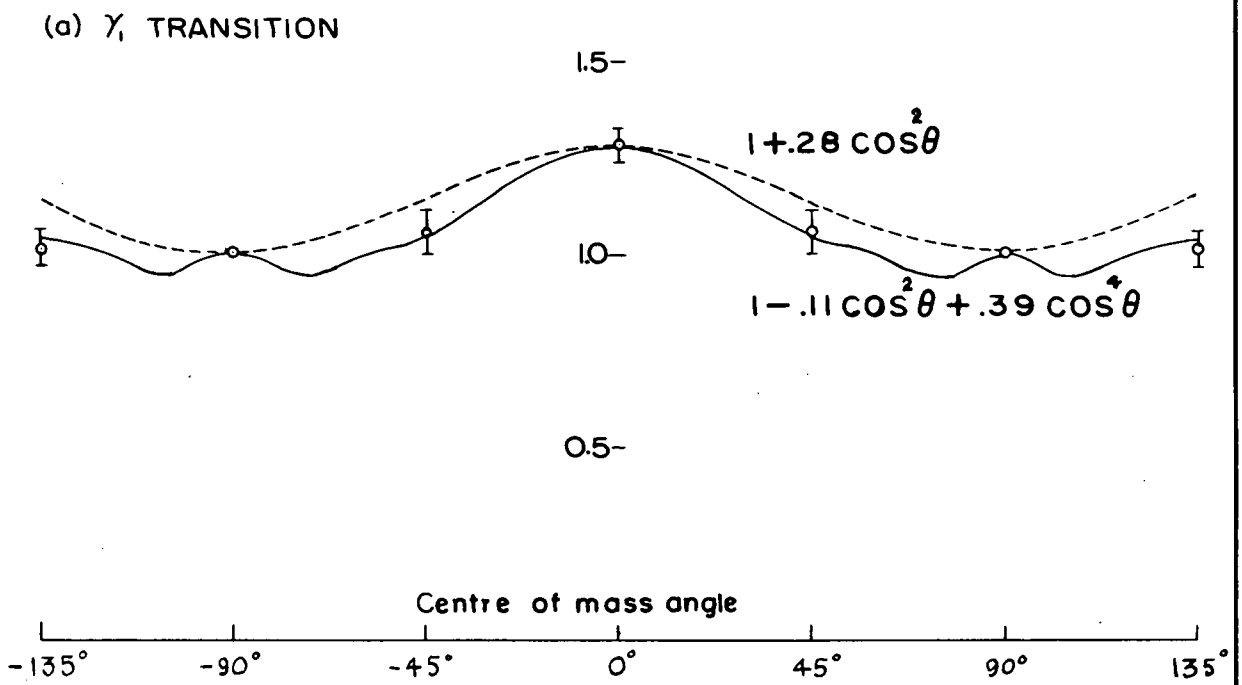

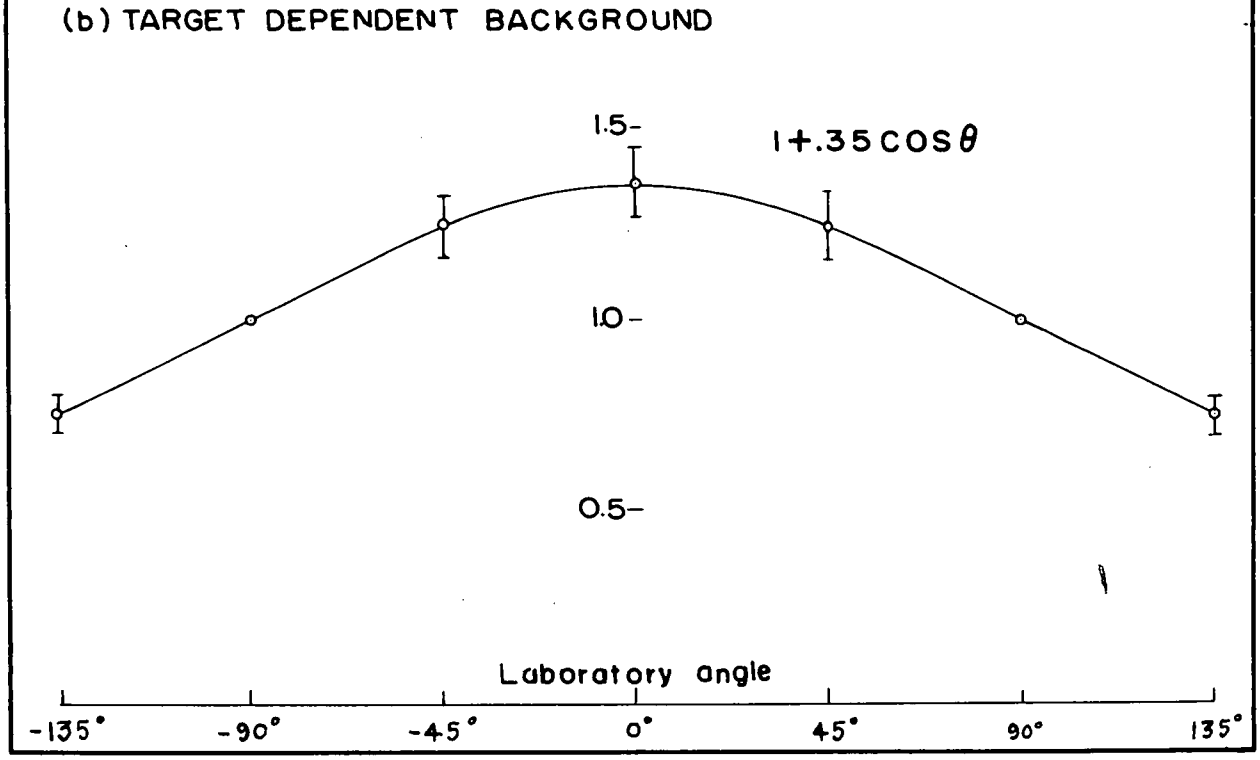

$\sigma_{c.m.}(\theta_{c.m.}) = \sigma_{lab}(\theta_{lab})\left[1-\frac{2v}{c}\cos\theta_{c.m.}\right]$ and $\theta_{c.m.} = \theta_{lab} + \frac{v}{c}\sin\theta_{c.m.}$

given by Devons and Hine (1949).

For a collision of an alpha particle of average energy $\bar{E}$ in Mev with a triton at rest the velocity of the pair after collision may be found as $v = 3.91\times10^{6}\sqrt{\bar{E}_{\alpha}}$ in metres per second. On the basis of these figures the corrections were calculated and found to change the above ratios by less than 3% and the angles by less than 1^{o}. The new values found were:

$\frac{N_{0^o}}{N_{90.8^o}} = 1.28\pm0.04$ $\frac{N_{45^o}}{N_{90.8^o}} = 1.06 \pm 0.06$ $\frac{N_{134.6^o}}{N_{90.8^o}} = 1.02 \pm 0.06$

These corrected values can then be fitted to an angular distribution of the form $\frac{N(\theta)}{N(90^o)} = 1+a\cos^2\theta + b\cos^4\theta$ with the result that a = -0.11 and b = 0.39. This distribution is shown in Figure 13 along with the corrected experimental results. For comparison the figure also shows the distribution which includes dipole terms only fitted to the values at 0^o and 90^o. This simpler type of distribution could only be fitted within the errors shown by assuming that all 45^o and 135^o points are low by an amount equal to or just greater than the errors shown on the individual points. It should be pointed out that the target dependent background which was left over after separating out the standard gamma ray spectra for γ_1 and γ_2 was not itself

isotropic. This point is discussed in more detail in section 4 of this chapter. It is felt that the decomposition proceedure used for the spectra has effectively removed any effect of the background anisotropy from the gamma ray angular distributions.

(ii) 800 Kev - Mean alpha energy in the target = 560 Kev.

At this energy measurements were made only at 0° and 90° which, after transferring to centre of mass co-ordinates, gave the average result, from about six runs, of $\frac{N0^\circ}{N_{90.7^\circ}} = 1.05 \pm 0.06$. Since this value is much closer to isotropic than that obtained at the higher bombarding energy and since the yield is considerably lower at this energy it was not considered worthwhile to make measurements at any further angles.

(f) Doppler Shift

The velocity of the alpha-triton pair after collision has been given previously as a function of mean alpha particle energy in the target: $v = 3.91 \times 10^6 \sqrt{\bar{E}_\alpha}$ in metres per sec. for $\bar{E}_\alpha$ in Mev. The values of $\bar{E}_\alpha$ appropriate have been given in section 2(b) of this chapter for the target at 45° to the beam. From theory the Doppler shift in energy for the detector at an angle θ with the beam is $E = E_0 \frac{v}{c} \cos\theta$. Measurements were made on with the results:

E_α	$\bar{E}_\alpha$	E_0	θ	ΔE Theory	ΔE Experiment
...	(Mev)	...	(degrees)	(Kev)	
1.6	1.32	3.03	0	44.8	42 ± 5

E_α	$\bar{E}_\alpha$	E_o	θ (degrees)	ΔE Theory	Experiment
			45	31.7	33
			90	0.0	0
			134	-32.2	- 30
0.8	0.56	2.71	0	31.4	28
			90	0.0	0

Within the experimental error the measurements are seen to agree with theory supporting the argument that the lifetime of the excited Li^7 nucleus to gamma ray emission is short compared to its slowing-down time in the target material.

4. Background

(a) General

After analyzing the $T(\alpha,\gamma)Li^7$ gamma ray spectra a smooth background remained as pointed out earlier. This target dependent background was from some material in the target itself other than any beam deposited carbon since it was present during early runs as well as later runs with about the same intensity. Also, it was noted that its general spectrum shape was similar to that seen by Larson (1957) when he looked at the low energy neutrons from the $D(d,n)He^3$ reaction with the $2\frac{1}{2}"x3\frac{1}{2}"$ NaI crystal.

Riley (1958) had observed that his target dependent background increased as the alpha particle bombarding energy

was decreased below 500 Kev and increased above 1.6 Mev. The shape of the $T(\alpha,\gamma)Li^7$ gamma ray spectra taken in the present work showed that the target dependent background decreased as energy decreased over the whole range studied. This background could have been due to the 14 Mev neutrons from the $T(d,n)He^3$ reaction caused by a small amount of molecular deuterium in the mass 4 beam, to neutrons of a few Mev energy from carbon buildup on the target, or from secondary neutrons produced by scattered tritium atoms in the target colliding with further target tritium atoms. Since it was therefore probable that neutrons were present it was decided to measure their energy, yield and anisotropy and to check whether they could possibly account for the anisotropic target dependent background found in the angular distribution runs.

(b) Energy of Neutrons

In order to roughly determine the energy of these neutrons from the target a beam of about $3\frac{1}{2}$ microamperes of alpha particles at 1.6 Mev was run on a thick tritium target (B-127-1) and the spectrum observed with a fast neutron counter of the type described by Ssu (1955). The photomultiplier of the counter was operated at 1275 volts obtained from an Isotopes Development E.H.T. supply. Pulses were fed from a cathode follower into a 100 ohm cable to a Dynatron Radio Limited Amplifier and from there to the 100-channel Computing Devices of Canada kicksorter. The kicksorter was operated at bias 1 to

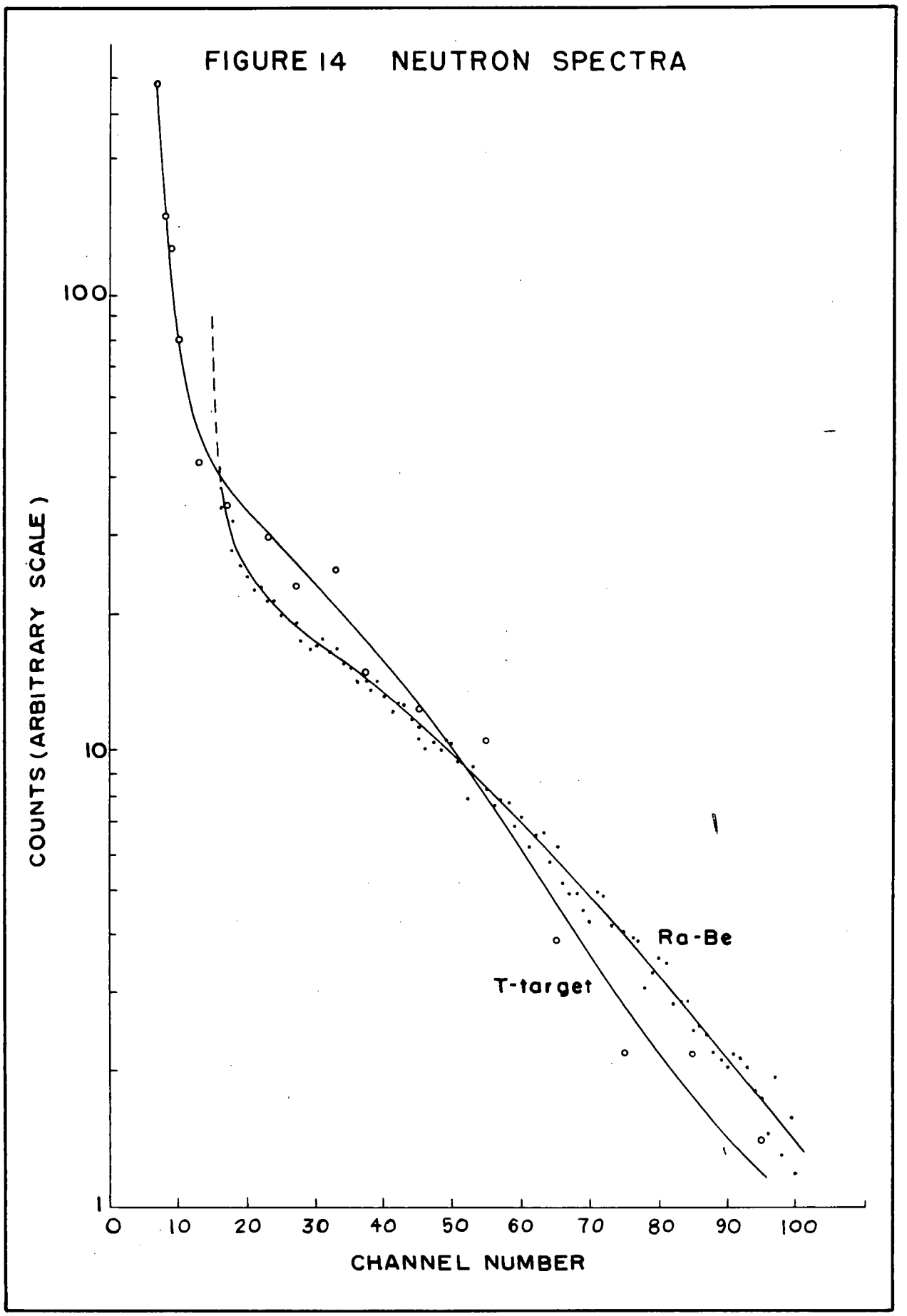
FIGURE 14 NEUTRON SPECTRA
100
10
1
COUNTS (ARBITRARY SCALE)
0
10
20
30
40
50
60
70
80
90
100
CHANNEL NUMBER
Ra-Be
T-target

observe the many low voltage pulses. A run of 150 integrators lasting over an hour was taken with the counter face as close as possible to the target pot. For comparison purposes a Ra Be neutron spectrum was obtained with the same counter, the kicksorter being at bias 2 to avoid the numerous pulses from gamma ray build up in the counter, with the gain otherwise the same. The two spectra are shown on a semi-logarithmic plot in Figure 14. By comparing the two curves with those given by Griffiths et al (1959) the energy of the neutrons from the target was seen to be about 2 to 3 Mev. This, therefore, ruled out the possibility of them being due to the $T(d,n)He^3$ reaction from molecular deuterium in the beam.

(c) Yield and Anistropy of Neutrons

On two separate occasions the anisotropy of the neutrons from the tritium target used for the $T(\alpha,\gamma)Li^7$ runs, when bombarded with 1.6 Mev alpha particles, was measured with the neutron counter mentioned above. Since these runs were not taken for a long enough time to accumulate many counts the pulses were not fed to the kicksorter being recorded only on a Dynatron Radio Limited scalar Type 1009A. Using the results of these runs the anistropy of the neutrons may be stated as

$$\frac{N_{0^\circ}}{N_{90^\circ}} = 1.32 \pm 0.3$$

From curves in the paper by Griffiths et al. the detector efficiency of the neutron counter for the neutrons

observed was believed to be about 0.2%. Assuming the effective centre of the counter to be 1" behind the front of the counter face and allowing 1-1/8" for the counter face-to-target distance the solid angle of the counter was calculated to be 0.7 steradian using a cross-sectional area of $20cm^2$. Then for N_c counts in the counter at 0^o per 50 integrator counts the number of neutrons emitted from the target per steradian at 0^o was $N_n = 708\ N_c$.

From a number of runs with the counter at 0^o the yield at 1.6 Mev and at 800 Kev alpha particle energies was found:

$E\alpha$ (Mev)	N_c	N_n
1.6	$150 \pm 15\%$	$1.06 \times 10^5 \pm 20\%$
0.8	$37 \pm 60\%$	$0.26 \times 10^5 \pm 65\%$

A yield at 800 Kev may therefore be given relative to that at 1.6 Mev as $\frac{Y(0.8)}{Y(1.6)} = 0.25 \pm 0.16$.

(d) Background Yield from the Scintillation Counter

In the gamma ray energy region from 2 to 3 Mev the target dependent background, resulting from analyses of $T(\alpha, \gamma)Li^7$ gamma ray spectra, was found to be always larger than the beam dependent one. When counts in this target dependent background were added from the half-energy bias of γ_1 to about 4 Mev the following yield rates were obtained for the counter at 90^o to the beam and for the bombarding energies shown in brackets:

$$\frac{Y(0.8)}{Y(1.6)} = 0.39 \pm 0.18 \qquad \frac{Y(0.5)}{Y(1.6)} = 0.37 \pm .017$$

It is therefore seen that the relative background yields at 500 Kev and 1.6 Mev as determined from gamma ray analysis agrees, within the experimented uncertainties, with that obtained from neutron counting thus lending support to the supposition that the target dependent background is neutron induced.

At 1.6 Mev alpha particle bombarding energy the total target dependent background for the counter at 90^{o} to the beam amounted to about 10,000 counts in 50 integrator counts. From the neutron counter results, assuming a scintillation counter solid angle of 0.18 steradian and a neutron anisotropy of 32%, the number of neutrons which entered the scintillation counter were: $N = \frac{1.06 \times 10^{5}}{1.32} \times 0.18 = 14{,}500$ neutrons. Thus, if neutrons in the NaI crystal are to be the explanation of the target dependent background then two out of every three neutrons entering the crystal must interact in some way. This proportion may be reduced, however, by considering the flux of gamma rays from the radiative capture of neutrons in the target pot and massive scintillation counter shielding.

(e) Angular Distribution

Counts in the target dependent background spectra in the scintillation counter which were left over after subtracting out γ_1 and γ_2 were added from the half-energy bias of γ_1 to about 4 Mev for $T(\alpha, \gamma)Li^{7}$ runs taken at different angles and at two energies in order to find the angular distribution of the back-

ground. Results may be stated in the laboratory system as

at E_α = 800 kev: $\frac{N_{0^o}}{N90^o} = 1.17 \pm 0.18$

at E_α = 1.6 Mev: $\frac{N_{0^o}}{N_{90^o}} = 1.36 \pm 0.10$ $\frac{N_{45^o}}{N_{90^o}} = 1.24 \pm 0.09$

$$\frac{N_{134^o}}{N_{90^o}} = 0.75 \pm 0.05$$

Applying a least squares fit to the data at E_α = 1.6 Mev for a function of the form $\frac{N(\theta)}{N(90^o)} = 1+a\cos\theta$ yields the result that a = 0.35 ± 0.9. This function is shown plotted in Figure 13.

It is interesting to note that the 0^o to 90^o anisotropy of this target dependent background was the same as that of the neutrons present thus further indicating that the background might have been produced by neutrons.

5. Absolute 90^o Differential Cross-Section

(a) Procedure

The runs for the determination of the absolute differential cross-section at 90^o to the beam direction were taken at the same time as the $T(\alpha,\gamma)He^4$ runs which have been used to determine the target thickness. To do these runs a relatively new spot on the target was selected and two $T(\alpha,\gamma)Li^7$ runs and two $T(p,\gamma)He^4$ runs were interspaced. No target deterioration was detected by this proceedure. For all of these runs the

scintillation counter was at 90° to the beam and 5.96 cm. from the outside of the target pot. The target was at 45° to the beam direction and positioned so that the gamma rays would pass through the target backing to reach the scintillation counter. The $T(\alpha, \gamma)Li^7$ work was done at an energy of 1.6 Mev as read by the generating voltmeter and with a target current of 4 microamperes. The spectra were analyzed into their two components as described before so that the cross-section could be given for γ_1 transitions. The tritium target thickness used was, as found from the $T(p, \gamma)He^4$ work, 4.48×10^{18} atoms/cm^2 $\pm$ 18% for the target at 45°.

(b) Cross-Section at 1.6 Mev

The efficiency of the scintillation counter in the lead castle for counts to the half energy bias of the spectrum was read from Figure 3 as $\epsilon = 0.68 \pm 5\%$ and the effective centre was used as 4.8 cm from the crystal face. After correcting for absorption losses the average number of $T(\alpha, \gamma)Li^7$ counts above the half-energy bias for γ_1 transitions, $N_c = 3240 \pm 5\%$. The rest of the data needed is as follows.

$\Omega = 0.179 \pm 6\%$

$$N_\alpha = \frac{(50 \text{ integrator counts}) \; 100.4 \times 10^{-6}}{1.6 \times 10^{-19}} = 3.137 \times 10^{16} \; \alpha\text{-particles} \pm 1\%$$

$n_T = 4.48 \times 10^{18}$ atoms of tritium/cm^2 $\pm$ 15%

$$\therefore \left(\frac{d\sigma}{d\omega}\right)_{90^\circ,\gamma_1} = \frac{N_c}{N_\alpha \, \Omega \, n_T \, \epsilon} = 1.89 \times 10^{-31} \text{ cm}^2/\text{steradian} \pm 20\%,$$

for the absolute 90° differential cross-section for γ_1 transitions. Using the ratio of γ_1 transitions to total transitions as 0.69 ± 0.007 then the absolute 90° differential cross-section for formation of Li^7 is found as

$$\left(\frac{d\sigma}{d\omega}\right)_{90^\circ} = \frac{1.89\times10^{-31}}{0.69} = 2.74\times10^{-31} \text{ cm}^2/\text{steradian} \pm 20\%$$

Integrating the angular distribution, $1-0.11\cos^2\theta + .39\cos^4\theta$, over 4π steradians yields a total cross-section for formation of Li^7 of

$$\sigma = 2.74\times10^{-31}\times(4.16\quad) = 3.58\times10^{-30} \text{ cm}^2 \pm 20\%.$$

(c) Excitation Function

Besides the 1.6 Mev bombarding energies two others were also used:

(i) 800 Kev

Unfortunately no 1.6 Mev runs were taken on the same spot on the target as 800 Kev runs. However, by examining the 800 Kev yield figures and those of runs at 1.6 Mev taken within a few days of these a reasonable cross-section can be given at 800 Kev relative to that at 1.6 Mev. The 800 Kev runs are those that were used in determining the angular distribution and as mentioned in that section the counter was appreciably closer than for the 1.6 Mev runs. In order to determine the relative cross-section at 800 Kev the following figures are used:

$$\left(\frac{d\sigma}{d\omega}\right)_{90^\circ, \gamma_1,\ 800\ \text{Kev}} = \frac{N_{\gamma_1},\ 800\ \text{Kev}}{N_{\gamma_1},\ 1.6\ \text{Mev}} \cdot \frac{N_\alpha,\ 1.6\ \text{Mev}}{N_\alpha\ \ 800\ \text{Kev}} \cdot \frac{\Omega_{1.6\ \text{Mev}}}{\Omega_{800\ \text{Kev}}} \cdot \left(\frac{d\sigma}{d\omega}\right)_{90^\circ, \gamma_1,\ 1.6\ \text{Mev}}$$

$$= \frac{2544}{3053} \cdot \frac{99.0}{102.5} \cdot \frac{0.179}{0.324} \cdot \left(\frac{d\sigma}{d\omega}\right)_{90^\circ, \gamma_1,\ 1.6\ \text{Mev}}$$

$$= 0.445 \left(\frac{d\sigma}{d\omega}\right)_{90^\circ, \gamma_1,\ 1.6\ \text{Mev}} \pm 11\%$$

or for the total cross-section $\sigma = 1.45 \times 10^{-30}\ \text{cm}^2 \pm 23\%$ assuming isotropy.

(ii) 500 Kev

An attempt was made to obtain a spectrum at 500 Kev incident alpha particle energy to note any change in target dependent background. At the time of running however, only a small current (2 μA) was available and this necessitated a long running time of about an hour for 75 integrator counts of 96.5 microcoulombs apiece. Over most of the spectrum the beam dependent background was more than half the number of counts recorded. However, a value was deduced for the cross-section relative to that at 1.6 Mev bombarding energy. Runs at 1.6 Mev on the same spot on the target had been taken just prior. Hence,

$$\left(\frac{d\sigma}{d\omega}\right)_{90^\circ, \gamma_1,\ 500\ \text{Kev}} = \frac{752}{3053}\ \frac{99.0}{96.5}\ \frac{0.179}{0.324}\ \left(\frac{d\sigma}{d\omega}\right)_{90^\circ, \gamma_1,\ 1.6\ \text{Mev}}.$$

$= 0.140 \left(\frac{d\sigma}{d\omega}\right)_{90,\gamma_1,\ 1.6\ \text{Mev}}$ ± 15%, or for the total cross-section, $\sigma = 0.50 \times 10^{-30}$ cm^2 ± 26% assuming isotropy.

(d) Target Thickness from Gamma Ray Energy

The gamma ray energies from the runs taken at the three bombarding energies followed a form $E_\gamma = Q + \frac{3}{7}\overline{E}_\alpha$, within the experimental accuracy, indicating that the proper reaction was being observed. From the RdTh energy calibrations the gamma ray energies were found and mean alpha particle energies calculated from them. These latter are compared with expected values, based on target thickness computations given in section 2(c), in the following tables:

E_α (Mev)	Target Angle (degrees)	$\overline{E}_\alpha$ Experiment (Mev)	From target-thickness (Mev)
1.6	45	1.31±10%	1.32
	90	1.37	140
0.8	45	0.567	0.560
0.5	45	0.355	

As can be seen the agreement is well within the experimental error and so mean alpha energies may be considered accurate to 2%.

6. Summary and Discussion of Experimental Results

The absolute cross-section for the $T(\alpha,\gamma)Li^7$ reaction was measured at 1.6 Mev alpha particle bombarding energy.

Values relative to this were found for energies of 800 and 500 Kev. Results are tabulated below for mean energies in the target:

$\overline{E_\alpha}$ (Mev)	σ_T (cm^2)	
1.32	3.58×10^{-30}	± 20%
0.56	1.45	23%
0.35	0.50	26%

These values are definitely lower than those of Riley but the relative values agree well with the trend of the cross-section with energy obtained by that author. On the other hand Holmgren and Johnston's values, obtained with a gas target, are lower by a factor of 2 at 600 Kev and a factor of 2.5 at 1.3 Mev and their excitation function falls less rapidly with energy. There is no immediately apparent explanation for this rather large discrepancy between the results determined by the two different methods at the present time.

Angular distribution measurements of the reaction gamma rays from $T(\alpha, \gamma)Li^7$ indicated that the gamma rays to the ground state, γ_1, and to the first excited state, , have the same angular distribution. These followed the form $1-0.11 \cos^2\theta + 0.39 \cos^4\theta$ at 1.6 Mev bombarding energy while there was some indication of anisotropy (5% ± 6%) at 800 Kev. The presence of the cosine terms at the high bombarding energy means that the reaction proceeds by capture of alpha particles of angular momentum greater than $l = o$ to some extent. If the

ground states of Li^7 are pure 2P levels then it is difficult to see how the quadrupole radiation, whose presence is indicated by the $\cos^4\theta$ term, arises since s, p, or d capture of alpha particles would give electric or magnetic dipole radiation.

The angular distribution of the target dependent background was found to be of the form $1+0.35\cos\theta$ at 1.6 Mev. This agreed well with anisotropy measurements made with a neutron counter. The excitation function of this background at 90° to the beam was determined roughly by measurements at 1.6 0.8 and 0.5 Mev. This also agreed very well with the neutron counter results. Therefore, indications are that the target dependent background was due to neutrons emitted from the target. One drawback to this however is that the yield of neutrons did not seem to be large enough to explain the large background in the scintillation counter. Further investigations to determine the exact source of the background would, therefore, be worthwhile.

7. Application of Results to Astrophysics

Because of the astrophysical interest in the absolute cross-section of the $T(\alpha,\gamma)Li^7$ reaction, as far as it determines the cross-section of the mirror reaction $He^3(\alpha,\gamma)Be^7$, the data was put in a form convenient for use. According to Burbidge et al (1957) the cross-section factor for a charged particle reaction in an energy region well below the coulomb

FIGURE 15 CROSS-SECTION FACTOR, S

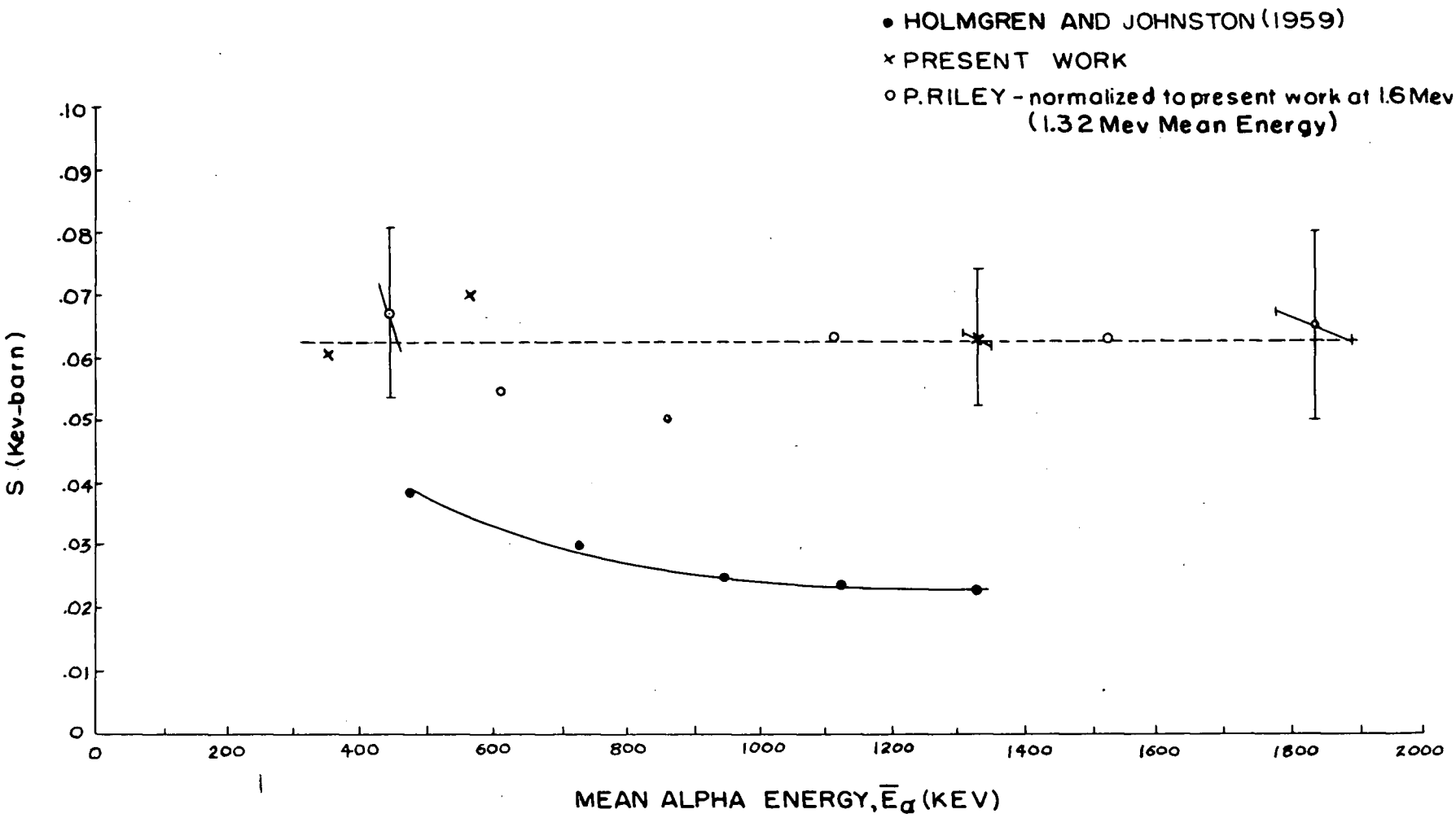

barrier may be written as

$S = \sigma(E_1)\, E_1 \frac{A_0}{A_0+A_1} \exp(31.28\, Z_1 Z_0 A_1^{\frac{1}{2}} E_1^{-\frac{1}{2}})$ Kev-barns in the centre-of-mass system, for E_1 the laboratory energy in Kev of the bombarding particle and $\sigma(E_1)$ the laboratory cross-section in barns (10^{-24}cm^2) for the reaction; A_0, A_1 refer to the mass of the interacting particles in atomic mass units and Z_0, Z_1, to their atomic number. For the $T(\alpha,\gamma)Li^7$ reaction this becomes $S = 3/7\ \bar{E}_\alpha\ \sigma(E_\alpha)\exp(125.12\bar{E}^{-\frac{1}{2}})$.

Using Riley's excitation function, normalized at $\bar{E}_\alpha$ = 1320 Kev to the absolute cross-section obtained from the present work the dependence of S on E_α was found. Riley's results were corrected for target thickness by using the stopping cross-section values from Figure 7 and the Oak Ridge National Laboratory's figure of 262 micrograms of Zr/cm^2 for his target.

The results of the present work and Riley's corrected results are shown plotted in Figure 15. Also shown are values of the same quantity as found by Holmgren and Johnston (1959) after converting their "S" to the centre of mass system. Within the experimental error the present results show that S does not change with energy in the region investigated. Holmgren and Johnston's results show a slow variation of S towards lower energies. This may be due to a small error in mean bombarding energy at the lower energies, which would result in a large

change in S because of its exponential dependence on $\bar{E}_\alpha$. The sloped lines through the experimental points show the direction in which S would vary with a slight change in mean bombarding energy. Over most of the energy range studied the best experimental estimate for S is 0.062 Kev-barn and it remains within about 25% of this value over the range.

If the reactions $T(\alpha,\gamma)Li^7$ and $He^3(\alpha,\gamma)Be^7$ were exact mirror reactions then the cross-section factors would be the same for both. On the assumption that they are exact mirror reactions cross-sections were found for the $He^3(\alpha,\gamma)Be^7$ reaction from those for the $T(\alpha,\gamma)Li^7$ reaction by multiplying the latter values by the factor $\exp(-125.12\bar{E}_\alpha^{-\frac{1}{2}})$ which results from the assumption of equal S values. Results are tabulated below as well as the cross-sections for the $He^3(\alpha,\gamma)Be^7$ reaction as found by Holmgren and Johnston.

Mean Energy $\bar{E}_\alpha$	$\bar{\sigma}$ $T(\alpha,\gamma)Li^7$	$\exp(-125.12E_\alpha^{-\frac{1}{2}})$	$He^3(\alpha,\gamma)Be^7$	Holmgren Johnston's $He^3(\alpha,\gamma)Be^7$
(kev)	($10^{-30}cm^2$)		($10^{-30}cm^2$)	($10^{-30}cm^2$)
350	0.50	0.124×10^{-2}	0.00062	----
430	0.89	0.240	0.0021	0.021
560	1.45	0.505	0.0070	0.078
610	1.3	0.628	0.0082	0.12
860	1.9	1.40	0.027	0.35
1105	3.1	2.32	0.072	0.75
1320	3.58	3.20	0.11	1.25
1520	3.9	4.04	0.16	----
1830	4.5	5.40	0.24	----

It is readily noticed that the cross-sections found from the $T(\alpha,\gamma)Li^7$ reaction are much lower than those obtained by

Holmgren and Johnston amounting to about a factor of 10 over the energy range studied. This indicates that the reactions $T(\alpha, \gamma)Li^7$ and $He^3(\alpha, \gamma)Be^7$ are not exact mirrors of each other. The two values of the cross-section would differ in the same direction if the repulsive force between the two protons in He^3 enlarged its radius over that of H^3 thus increasing the cross-section of the $He^3(\alpha, \gamma)Be^7$ reaction.

Part II

A Standard Geiger-Muller Counter for Gamma Ray Flux Determinations

Chapter I

Introduction:

The Geiger-Muller counter, as all other nuclear radiation detectors, depends on the ionizing power of the radiation for its operation. By means of gas amplification it amplifies the primary ionization, caused by the radiation in its interior, and the resultant flow of charge, is practically independent of the number of ions originally formed.

The term, Geiger counter, actually refers to a point counter as originally designed by Geiger (1913). This consists of a thin wire at high potential surrounded by a metallic cathode; the interior is gas filled. Gas amplification takes place around the point of the wire in the gaseous atmosphere resulting in a collected charge independent of the amount of original ionization. A slight modification of this made by Geiger and Klemperer (1928) was to add a small metal ball to the end of the wire. Over a small voltage range this device operates as a proportional counter--the amount of charge collected on the wire being proportional to the original number of ions formed. Thus, charged particles give a voltage pulse proportional to their energy. Since the above counters operate

only around the end of the wire the active volume is small. In order to increase the sensitive volume a new counter was developed (Geiger and Muller, 1928) known as the Geiger-Muller or G-M counter. In this device amplification of ionization occurs along the complete length of the high voltage wire thus giving greater sensitivity.

Since gamma rays are detected by the ionization resulting from electrons liberated from the materials of the counter a good gamma ray G-M counter should have a large solid surface area surrounding the gas-filled interior. Because these secondary electrons have a finite range in the cathode material the wall thickness should be just greater than this range to ensure that the maximum sensitivity is obtained. If the walls are thicker than this then sensitivity is lost as a result of gamma ray absorption in the walls which can not contribute electrons to the interior. Primary ionization in the gas may be considered negligible (Bleuler and Goldsmith, 1952). Even a wall thickness of the order of a millimetre stops all beta and alpha particles ensuring that only gamma rays and X-rays are detected.

Fowler et al. (1948) as well as other authors (Bleuler and Zunti, 1946) have made elaborate theoretical calculations in the efficiency of a thick walled G-M counter. In their paper they find that the gamma sensitivity varies essentially

linearly with photon energy for an aluminum cathode between 1.5 and 25 Mev; at the lower energies the efficiency changes less rapidly with energy.

An approximate expression for the overall efficiency was given by von Droste (1936) as ϵ = Constant ($\sigma_{ph}\ t_{ph} + \sigma_c\ t_c + 2\sigma_p\ t_p$) where σ_{ph} is the cross-section for the photoelectric effect, t_{ph} is the range of the secondary electrons in the wall material and the other symbols have analagous meanings.

This formula predicts that the efficiency at energies below about 300 Kev increases significantly rather than smoothly falling to zero with decreasing photon energy. This effect is due to the nature of the photoelectric cross-section at these low energies and has been born-out in the experimental results of Bradt et al. (1946) and Dunworth (1940).

Since the photoelectric effect depends on Z^4, pair production on Z^2 and the Compton effect on Z high sensitivity to gamma radiation is gained by employing cathode materials of high atomic number, Z.

Although G-M counters do not occupy the same position as they did ten years ago for gamma ray flux measurements it was felt that an experimental determination of their efficiency over a wide range of photon energies would be worthwhile not

only to make available a standard counter for determining gamma ray fluxes in the laboratory but also as an independent check on the flux measurements made with scintillation counters. Accordingly efficiencies have been found for a standard brass (Z = 29) walled counter over the gamma ray energy range from 0.5 Mev to 20 Mev.

Efficiency determination at 6.14 Mev and 17.6 Mev gamma rays for a similar counter were made a few years ago by Barnes et al (1952); this present work is an extension of theirs.

Chapter II

Determination of Characteristics:

1. Method of Operation

When a gamma ray enters the counter wall there is a certain probability depending on the gamma ray energy and the counter construction of it interacting and producing electrons by one of the three effects: Compton, photoelectric or pair production. These electrons, if produced near enough to the inner surface of the wall, will reach the gaseous interior. Here they will be accelerated by the potential gradient between the thin wire anode and the counter wall and will ionize the gas by collisions producing electron-ion pairs. These electrons, in turn, produce more ionization and successive collisions in the region of the counter wire and initiate an electron avalanche which spreads along the wire. The production of new avalanches ceases when the positive ion sheath moving slowly towards the cathode reduces the field at the anode to such an extent that no further multiplication can occur. Thus, at this time, a fraction of a microsecond after the passage of the primary particle the primary discharge is terminated. If the ion sheath, which takes from 100 to 500 microseconds to cross the counter volume, is allowed to strike the cathode it produces photons which eject electrons by the photoeffect thus initiating a new discharge. In order to prevent this multiple discharging which occurs with counters using pure gases quenching can be accom-

FIGURE 16 STANDARD G-M COUNTER

Drawing to scale:

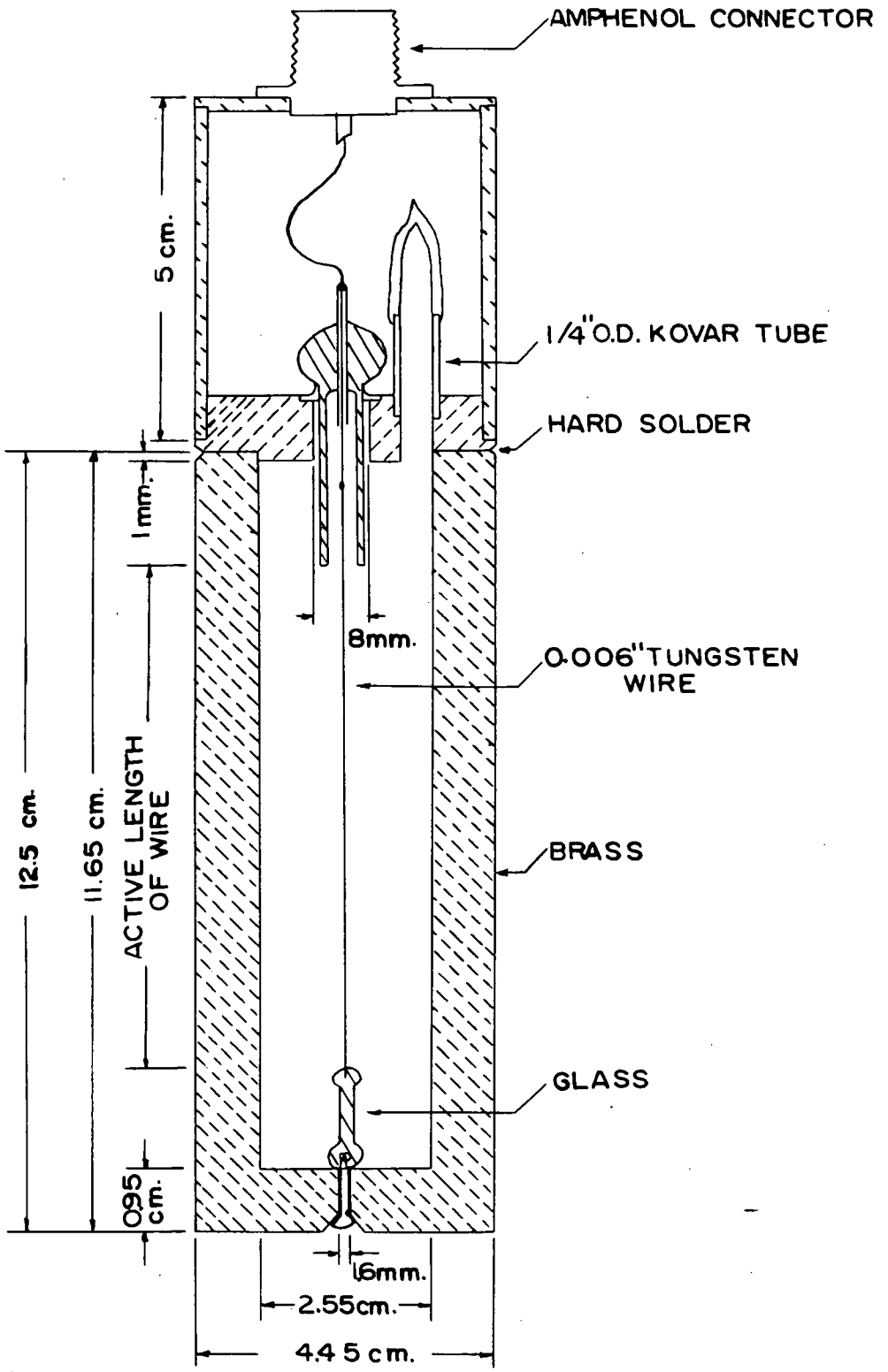

plished by proper electronic circuitry (Bleuler & Goldsmith, 1952) which reduces the high voltage across the counter for a short period after each discharge. Alternatively, instead of a pure counter gas, such as argon, a small amount of polyatomic vapor, such as alcohol, may be added to serve as a quench gas. This gas mixture does not affect the initial production, however after the discharge instead of the positive argon ions hitting the cathode they collide with alcohol molecules, thereby transferring their charge to these heavy molecules. The alcohol molecules then move towards the cathode and dissociate upon hitting it rather than emitting an electron. Due to the dissociation of the quench gas the lifetime of the counters is limited; counter life is usually of the order of 10^8 to 10^{10} counts.

2. Construction and Filling

A sectional diagram showing the construction of the Geiger-Muller counter used for the efficiency determinations is shown in Figure 16. It consisted of a piece of brass tubing of 4.45 cm. outside diameter of 0.95 cm. wall thickness closed at the ends. Glass-to-metal seals at both ends keep the high potential 0.006 inch diameter tungsten wire insulated from the counter walls. A glass sleeve at the entrance end serves to define the active length of the wire more accurately by keeping the active volume away from the brass end of the counter where the field is non-uniform. This particular counter was designated

FIGURE 17 COUNTER FILLING SYSTEM

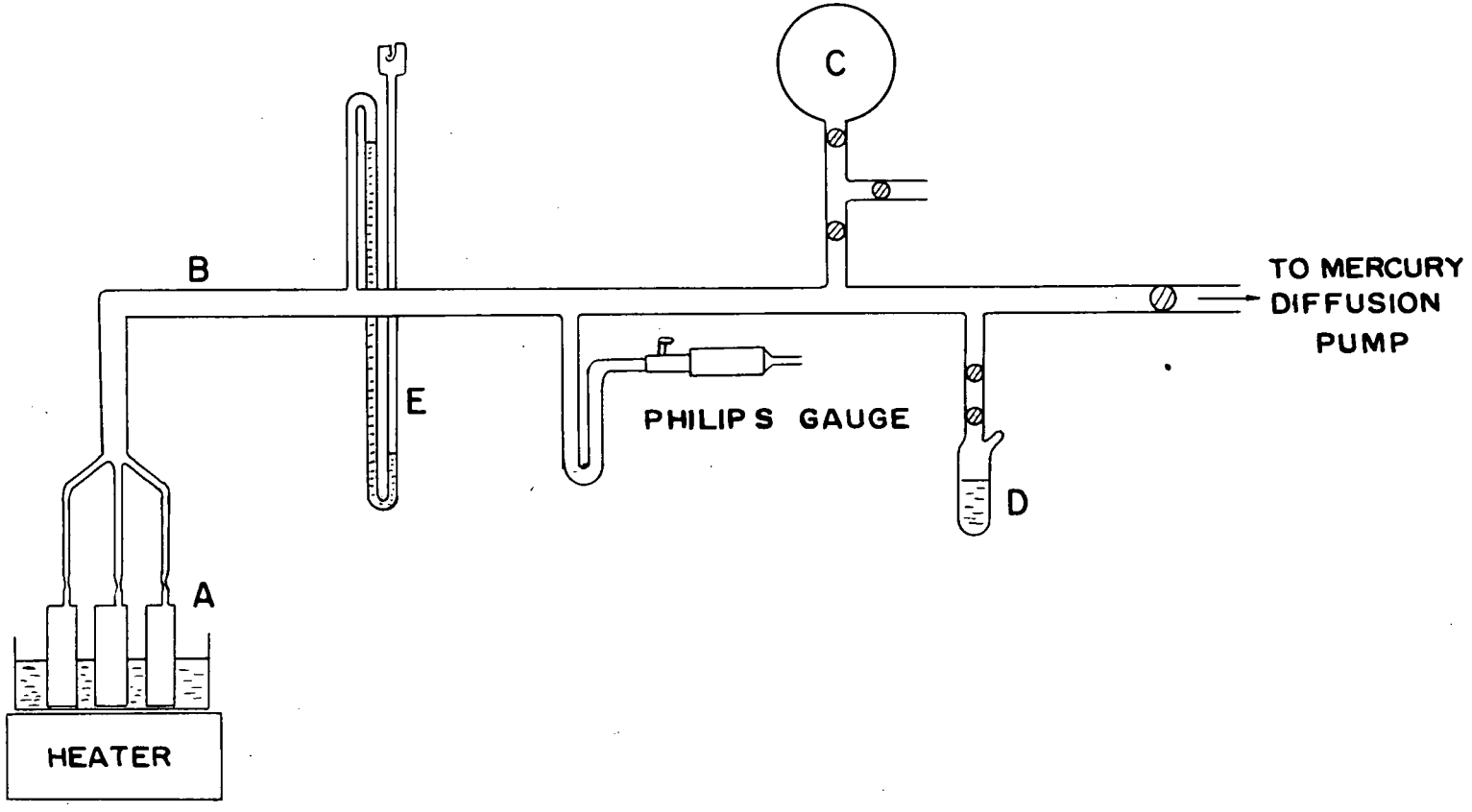

as Mark I. A slightly different construction was used in two later counters referred to as Mark II Nos. 1 and 2. Active lengths, as defined in the figure were measured for the three counters:

Counter	Length (cm)
Mark I	7.5
Mark II No. 1	7.36 ± 0.08
Mark II No. 2	7.58 ± 0.08

The counters were filled by the usual method (Bleuler and Goldsmith); the filling system is shown in Figure 17. Filling proceedure was as follows: the G-M counters A were sealed to the manifold B and the system pumped down with the mercury diffusion pump. The evacuation continued while the counters were warmed in hot water to outgas them. Pumping continued this way for a number of hours until little increase above the normal 10^{-4} mm. Hg pressure was noticed when the system was sealed off from the pumps and the hot water removed from the counters. The tube was then flushed with argon from the flask C. After closing C the pumping line was opened and the pressure allowed to fall to nearly its original value where the evacuation was stopped. Alcohol from the bottle D was then evaporated into the system until the pressure rose 1 cm. as read by the mercury manometer, E. The alcohol was then closed off and argon introduced, letting the pressure climb to 11 cm. After sitting a few hours in this condition so that uniform mixing of

gases occurred counter plateaux were obtained. Finding these satisfactory the counters were removed from the system.

3. Plateau and Resolving Time

Immediately after the counters had been removed from the filling system another check on their characteristics was made using a Berkely Model 2105 Decimal Scalar and a Co^{60} source of gamma rays. The G-M pulses were viewed concurrently with an oscilloscope; both scalar and oscilloscope agreed as to where the Geiger threshold was. Plateau characteristics are given below for two of the G-M counters immediately after filling and after about nine months of use:

Counter	After Refilling		After Use	
	Length	Slope	Length	Slope
Mark I	300	0.05/100	150	0.08/100
Mark II, No. 1	200	0.06/100	200	0.08/100

A counter is considered satisfactory if the plateau is 200 to 300 volts long and has a slope of about 0.05/100 .

The two source method was employed to find the resolving time of the Mark I counter (Bleuler and Goldsmith). For this, two Co^{60} gamma ray sources were used with the results:

m_{12} = observed count rate for two sources = 20,956 $\pm$ 64 per min

m_1 = " " " " source 1 only= 9,100 $\pm$ 42 " "

m_2 = " " " " " 2 " = 12,672 $\pm$ 50 " "

m_b = " " " " no source = 35.8 $\pm$ 1.4 " "

Then the resolving time is determined from

$$\tau = \tau_1 \left[1 + \frac{\tau_1}{2}(m_{12}-3m_b)\right] \text{ and } \quad \tau_1 = \frac{m_1+m_2-m_{12}-m_b}{2(m_1-m_b)(m_2-m_b)}$$

giving τ = 212 microseconds $\pm$ 5%. This is a typical value for a G-M counter.

4. G-M Counter Efficiency

(a) Definition of Efficiency

The overall sensitivity or efficiency, ϵ, of a Geiger-Muller counter can be defined by the formula $N_G = \frac{A\epsilon}{4\pi r^2} N_\gamma$

where N_G = number of counts in the G-M counter

N_γ - corresponding number of gamma rays emitted from the source

r = distance from the source to the effective centre of the counter

A = effective area of the counter.

The factor $\frac{A}{r^2}$ may be considered to be the solid angle of the counter and an analytical expression for it in terms of counter dimensions is given by Norling (1941). However, in this present work A was taken together with ϵ and an "effective efficiency" $A\epsilon$ defined. Such an efficiency is, therefore, characteristic of the counter under investigation.

If counts are recorded at a number of distances from the source then a plot may be made of $\sqrt{\frac{N_\gamma}{N_G}}$ versus r, and a

straight line of slope $m = \frac{1}{r}\sqrt{\frac{N_\gamma}{N_n}}$ should result so that the effective efficiency is $A\epsilon = \frac{4\pi}{m^2}$. An effective centre distance for the counter may also be found by noting the intercept on the r axis.

In analyzing the results a least squares line $Y = mx+b$ was fitted to the inverse square law plot and the slope and intercept found as

$$m = \frac{n\sum_i x_i\ y_i - \sum x_i\ y_i}{n\sum_i x_i^2 - \left(\sum_i x_i\right)^2} \quad \text{and} \quad e = \frac{b}{m} = \frac{\sum_i y_i - m\sum x_i}{nm}$$

where n was the number of independent observations. An estimate of the error involved for m and b was found by a method described in Whittaker and Robinson (1924) and outlined here:

The condition that the least squares line must satisfy may be written in two "normal" equations:

$$[xx]m + [x1]b = [xy]$$

$$[x1]m + [11]b = [1y]$$

where $[xy] = \sum_i x_i\ y_i$

If D is the determinant of the coefficients in these equations and $\delta^2 \equiv [\delta\delta] = [yy]-[xy]m-[1y]b$ then the quadratic mean errors associated with m and b are

$$\delta^2_m = \frac{[11]}{D}\cdot\frac{\delta^2}{n-2} \quad \text{and} \quad \delta_b^2 = \frac{[xx]}{D}\cdot\frac{\delta^2}{n-2}$$

FIGURE 18 CIRCUIT CONNECTIONS

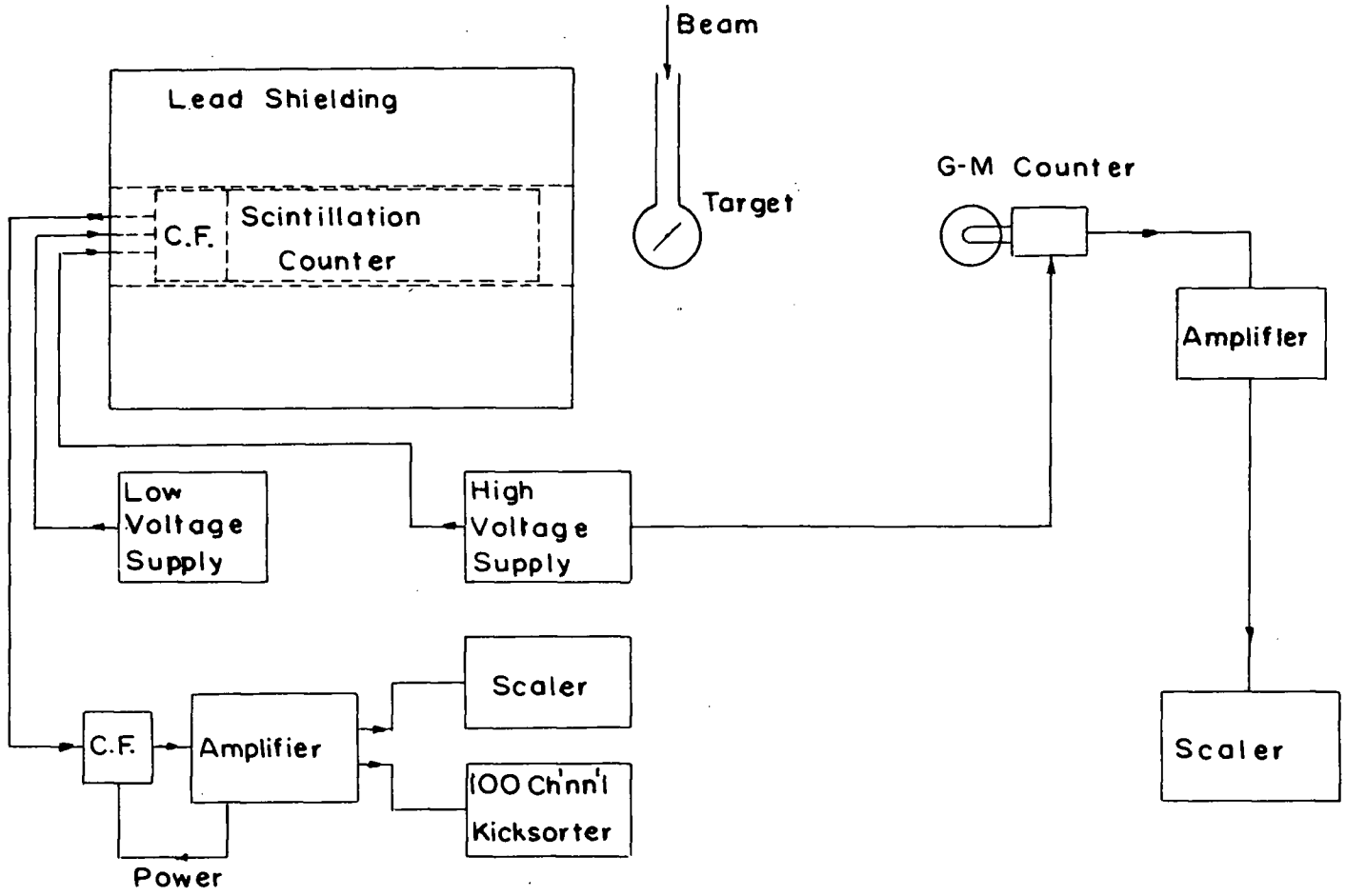

(b) Experimental Proceedure

The G-M counter efficiency was determined by applying the theory of the last section to data taken at six different gamma ray energies. The mean energies used were 0.51, 1.25, 6.16, 12.1, 16.3, and 20.3 Mev from the reactions $Na^{22}(\beta+)Ne^{22*}$, $Co^{60}(\beta^-\gamma)Ni^{60}$, $F^{19}(p,\alpha\gamma)O^{16}$, $B^{11}(p,\gamma)C^{12}$, $Li^{7}(p,\gamma)Be^{8}$ and $T(p,\gamma)He^{4}$ respectively.

A block diagram of the G-M counter circuit connections is shown in Figure 18. Geiger pulses were fed through an Atomic Instrument Co. Linear Amplifier Model 403-B into a 100 ohm cable to a Dynatron Radio Ltd scalar Type 1009A. High voltage for the G-M counter was 1175 volts from an Isotopes Development E.H.T. supply. This resulted in an overvoltage of about 125 volts putting the operating point around the centre of the plateau.

For runs involving a scintillation counter (either the $2\frac{1}{2}$"x$3\frac{1}{2}$" crystal or the $2\frac{3}{4}$"x$4\frac{1}{2}$" crystal) the circuit connections for this counter were also as shown in the figure. Pulses were fed from the output cathode follower unit mounted on the scintillation counter through a 100 ohm cable to a cathode follower and hence to a Dynatron Radio Ltd Amplifier Type 1430A. Positive pulses from this unit drove a Dynatron Radio Ltd scalar Type 1009A in parallel with the 100 channel Computing Devices of Canada Ltd. kicksorter. Calibration of the system was carried out as described in Part I.

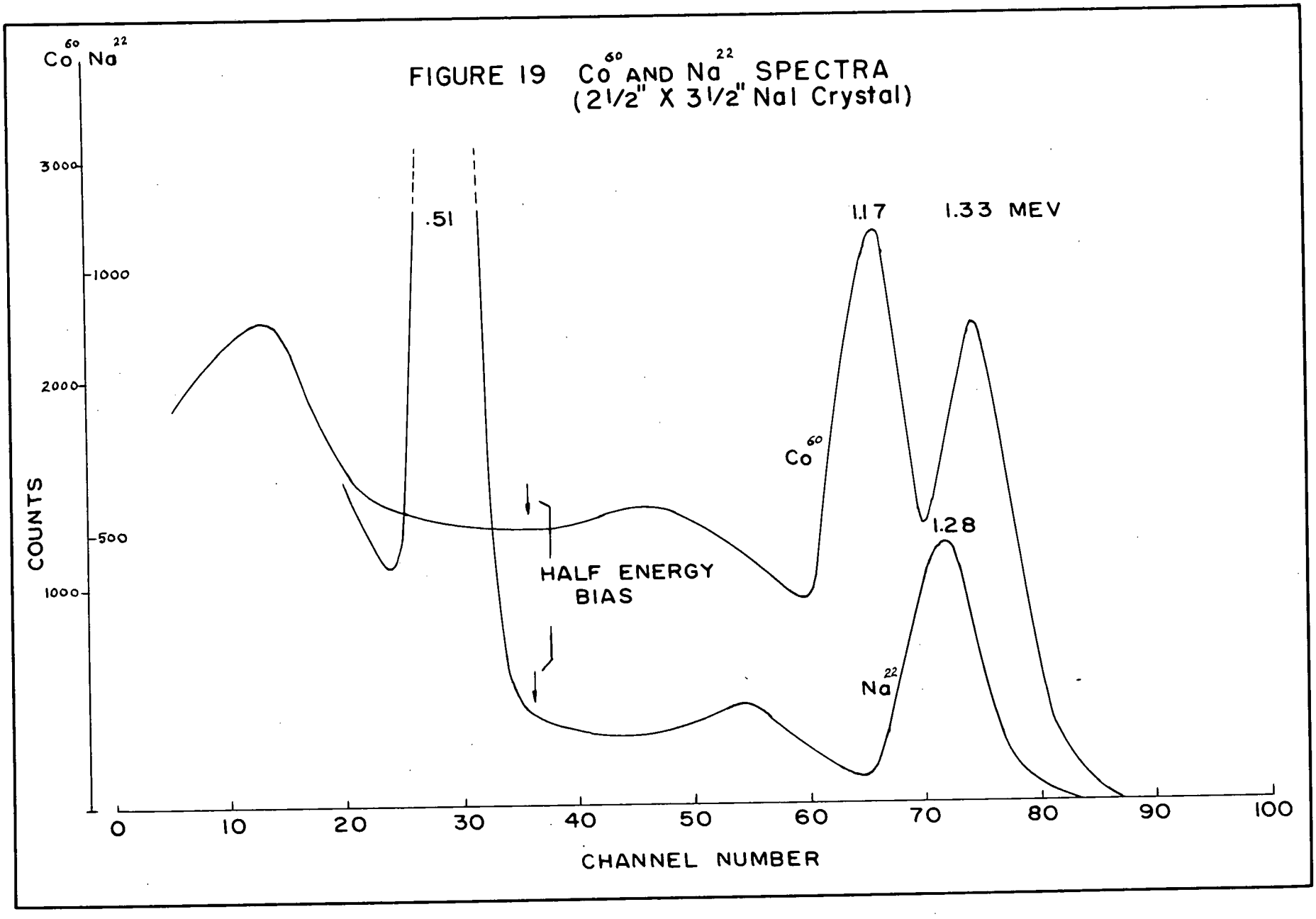
Co 60 Na 22
FIGURE 19 Co 60 AND Na 22 SPECTRA
(2 1/2" X 3 1/2" NaI Crystal)
3000
1000
2000
500
1000
COUNTS
.51
1.17
1.33 MEV
Co 60
1.28
HALF ENERGY
BIAS
Na 22
0
10
20
30
40
50
60
70
80
90
100
CHANNEL NUMBER

(c) Procedures at 0.51 Mev

In the decay of Na^{22} a positron is emitted in 89% of the cases (Kreger, 1954) and an electron is captured in the remaining ones resulting in an excited state of Ne^{22} of 1.275 Mev (Ajzenberg and Lauritsen) which decays with a half-life of 4.8×10^{-12} second (Alkhazov, D.K. et al., 1959). The radiation from the annihilation of the position was used to determine the G-M counter efficiency at this 0.51 Mev photon energy. The number of 0.51 Mev gamma rays was 1.78 times the number of 1.28 Mev gamma rays.

In order to determine the absolute strength of Na^{22} activity the spectrum of the 1.275 Mev gamma ray shown in Figure 19 was recorded with the $2\frac{1}{2}$"x$3\frac{1}{2}$" NaI crystal mentioned in Part I and the number of counts above the half-energy bias compared with the analagous number in the spectrum also shown in the figure of 1.17 and 1.33 Mev gamma rays from an accurately known Co^{60} source. Fortunately the mean Co^{60} gamma ray energy is almost exactly the same as the Ne^{22} 1.28 Mev gamma ray so that the scintillation counter efficiency is the same in both cases the ratio of Na^{22} counts to Co^{60} counts was found to be, $R=0.110 \pm 1.2\%$ on December 31, 1958. This ratio has been corrected for the loss of counts due to the kicksorter resolving time of (30 + channel number) microseconds. The sources used were Na^{22} #2 and Co^{60} #1. This latter source had been calibrated by the National Research Council of Canada on April 11, 1956 as having

a strength of 0.031 millicuries within 5%. P.P. Singh of this laboratory using coincidence techniques on the two cascade gamma rays had found the activity to be 0.0237 millicuries within 3% on April 22, 1958, in agreement with the previous measurement assuming a Co^{60} half-life of 5.2 years. Taking account of the fact that one disintegration of a Co^{60} nucleus results in two gamma rays, the strength of the Na^{22} #2 source, on December 31, 1958 was 0.00432 millicuries $\pm$ 5% for the 1.27 Mev gamma rays.

To do the efficiency measurements the G-M counter was held about three feet off the floor with its axis vertical and counts were taken for Na^{22} source-to-counter distances, r, from 15 cm. to 40 cm. The proceedure was then repeated with the Co^{60} source for the same counting time and distances. If N_{22} is the number counts due to the Na^{22} source and N_{60} is the analagous number from the Co^{60} source then the counts due to the 0.51 Mev gamma ray are $(N_{22}-k\ N_{60})$ and the effective efficiency at 0.51 Mev is found from $A\epsilon = \frac{\pi r^2}{0.89k\ N} \cdot (N_{22}-k\ N_{60})$ where N is the number of disintegrations of Co^{60} nuclei in the counting time. Efficiencies and effective centres for both Mark I and Mark II, No. 1 counters were measured in this way.

(d) Procedure at 1.25 Mev.

When a Co^{60} nucleus decays two gamma rays of energy 1.17 and 1.33 Mev are emitted in cascade. The G-M counter efficiency was assumed to vary linearly between these two energies

so that a mean energy could be defined as 1.25 Mev. The data obtained with the Co^{60} source in the previous section was used for the determination of the effective efficiency and effective centre at this energy. For N_γ, the number of disintegrations of Co^{60} nuclei in the counting time, the efficiency is given by $A\epsilon = 2\pi r^2 \frac{N_{60}}{N_\gamma}$.

(e) Procedure at 6.16 Mev

A CaF_2 target mounted in the target chamber described by Larson (1957) was bombarded with 365 Kev protons. The protons were captured in the 340 Kev resonance and a highly excited state of Ne^{20} was formed. This decayed mainly to the 6.14 Mev level of O^{16} by the emission of an alpha-particle. Other states at 6.91 and 7.12 Mev were formed in 2.3% ± 0.2% of the decays (Dosso, 1957). The mean gamma ray energy for the G-M counter efficiency determination was therefore 6.16 Mev.

The isotropically emitted alpha-particles (Devons and Hine 1949) to the 6.14 Mev state were counted by a proportional counter in an accurately known geometry: $\omega = (2.357 \pm 0.005) \times 10^{-5}$ of a sphere. From the alpha counts the number of gamma rays emitted isotropically could be found as $N_\gamma = \frac{\alpha \text{ counts}}{\omega} \times (1.023 \pm 0.002)$.

The G-M counter was held with its axis vertical and positioned so that the gamma rays from the target would pass

perpendicularly through the thin copper target backing and the one millimetre thick aluminum window to reach it. The counter-to-target distance was varied from about 20 cm. to 60 cm. Pulses from the proportional counter were amplified by a Dynatron Radio Limited Amplifier Type 1430A and recorded on the 100 channel kicksorter in parallel with a Dynatron Radio Ltd scalar Type 1009A.

For a count N_G in the G-M counter corresponding to N_γ gamma rays emitted the effective efficiency was found simply as $A\epsilon = 4\pi r^2 \frac{N_G}{N_\gamma}$

Again, efficiencies and effective centres were calculated for Mark I and Mark II, No. 1 G-M counters.

(f) Procedure at 12.1 Mev

By bombarding a B^{11} target with 275 Kev protons gamma rays of energies 4.43, 11.67 and 16.10 Mev were emitted (Ajzenberg and Lauritsen, 1955). At this proton energy the 16.0 Mev contribution was small but not negligible.

A B^{11} target was mounted in a 3.65 cm outside diameter 1/16" brass walled target pot. The Mark I G-M counter and the scintillation counter with the $2\frac{3}{4}$"x$4\frac{1}{2}$" NaI crystal were positioned at 90° to the proton beam. The front face of the scintillation counter was located 15 cm from the outside of the target pot while the G-M counter-to-target distance was varied from about 5 cm to 40 cm.

FIGURE 20 SPECTRA OF $B^{11}(p,\gamma)C^{12}$ GAMMA RAYS
(in 2 3/4" X 4 1/2" NaI Crystal)

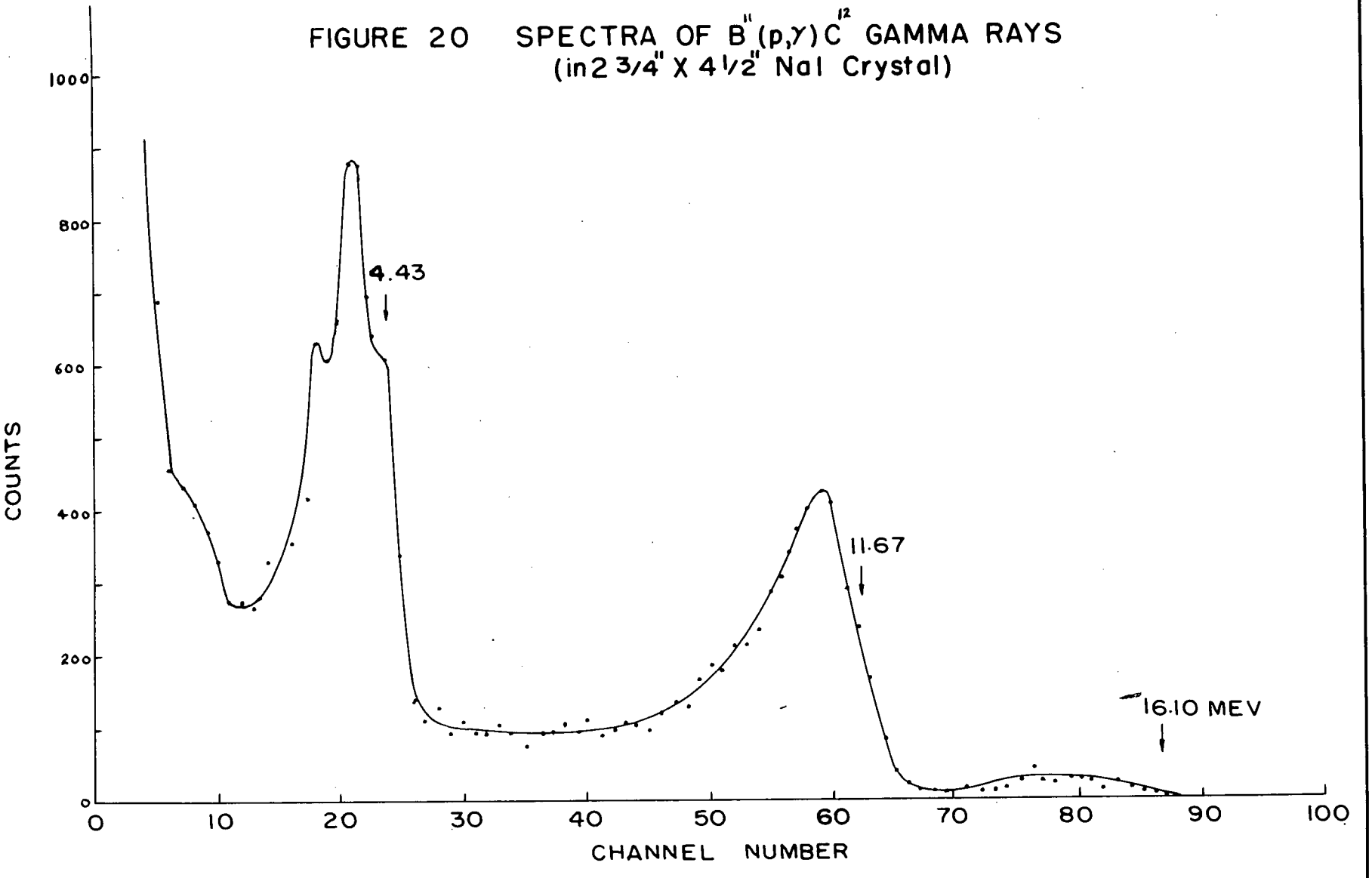

A typical spectrum obtained in the scintillation counter is shown in Figure 20. The number of gamma rays of each energy emitted in the 90^{o} direction was found by determining the number of counts above the half-energy bias in the scintillation counter spectra and using a scintillation counter efficiency as read from Figure 3. The efficiencies and effective centre distances used were 0.705, 0.790, 0.798 and 4.6 cm., 4.1 cm., 4.1 cm. for gamma ray energies of 4.43, 11.67 and 16.10 Mev respectively.

From previous results an efficiency for the 4.43 Mev gamma ray in the G-M counter was found from interpolation; the value taken was $(A\epsilon)_4 = 0.59$. Using this efficiency and the intensity of 4.43 Mev gamma rays incident in the direction of the G-M counter as determined from scintillation counter spectra the 4.43 Mev gamma ray contribution to the counts in the G-M counter was determined. The remaining counts were then due to the 11.67 and 16.10 Mev gamma rays. From their relative intensities in the scintillation counter a mean energy for use with the G-M counter was calculated to be 12.1 Mev. Hence the effective efficiency for 12.1 Mev photon energy was inferred from:

$$\left[N_G - \frac{(A\epsilon)_4 \quad N_4}{4\pi r^2}\right] = \frac{1}{4\pi r^2} \quad (A\epsilon)_{12} \left[N_{12} + N_{16}\right]$$

where N_E was the number of gamma rays of energy "E" Mev being emitted from the target as found from the scintillation counter spectra and assuming isotropic distribution.

FIGURE 21 SPECTRA OF $Li^{7}(p,\gamma)Be^{8}$ GAMMA RAYS
(in 2 3/4" X 4 1/2" NaI Crystal)

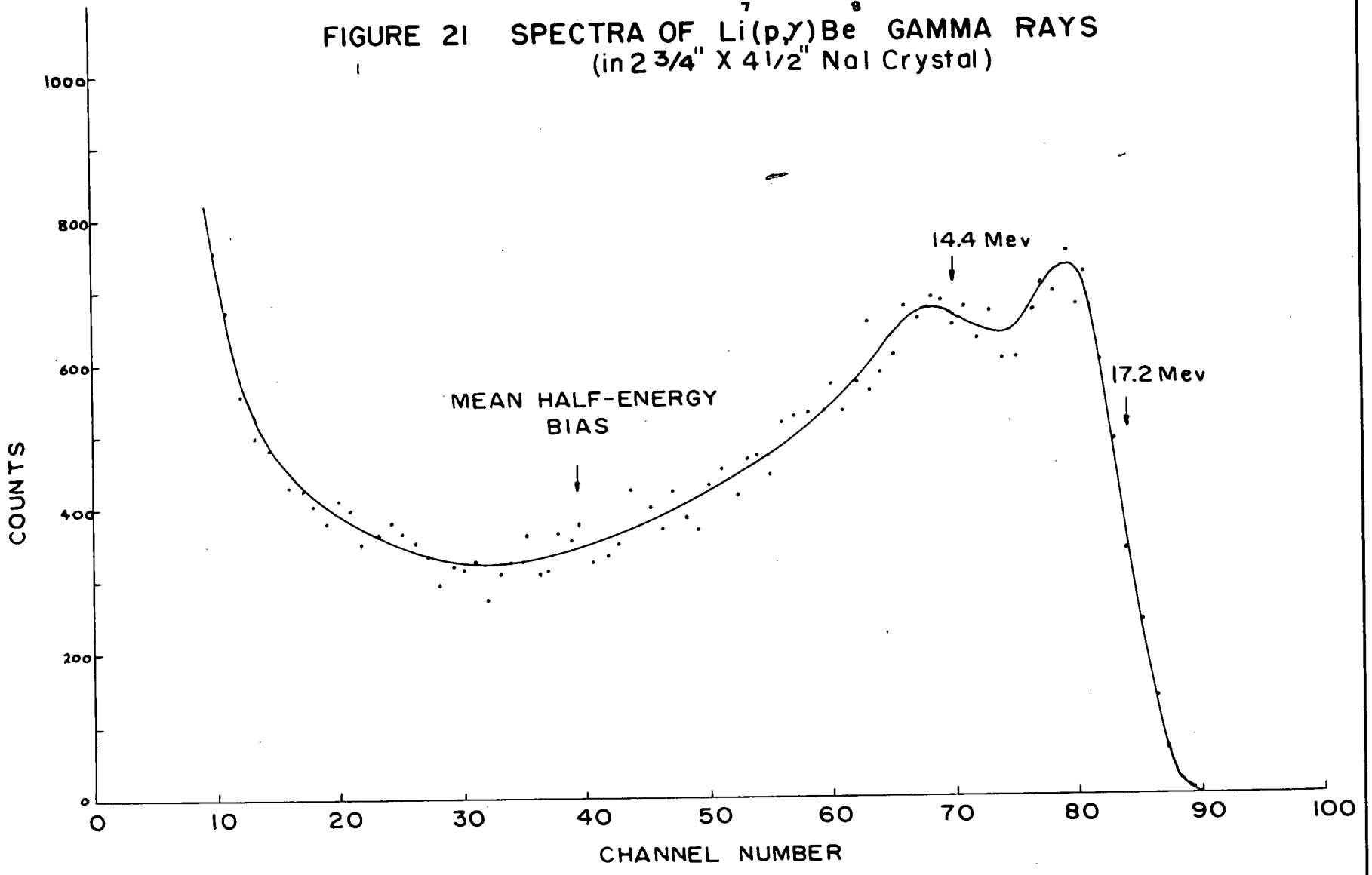

(g) Procedure at 16.3 Mev

A thin Li^7 target evaporated onto a copper backing by the method described by Singh (1959) was bombarded with 450 Kev protons. The protons were captured in the 4.41 Kev resonance of Be^8. In the subsequent decay a 14.4 or a 17.2 Mev gamma ray was emitted (Ajzenberg and Lauritsen, 1955) both being separately isotropic (Devons and Lindsey, 1950). Since their relative intensities were 2:1 (Walker and McDaniel, 1948), the 17.2 Mev gamma ray being the more intense, a mean photon energy was found as 16.3 Mev.

The large scintillation counter, used for the measurements at 12.1 Mev, was positioned at 90° to the proton beam, its front face being 29.65 cm. from the outside of the 2" diameter brass walled target pot mentioned in Part I. The Mark I G-M counter was located opposite the scintillation counter also at 90° to the beam. Its distance from the target was varied from about 5 cm to 40 cm. A typical spectrum obtained in the scintillation counter is shown in Figure 21. The total number of gamma rays emitted N_γ was found by adding counts in the spectra from a weighted half-energy bias and using a mean scintillation counter efficiency of 0.797 from Figure 3. The effective centre distance used was 4.1 cm. Thus, a G-M counter efficiency at 16.3 Mev was found simply from $N_G = \frac{A\epsilon}{4\pi r^2} N_\gamma$.

(h) Procedure at 20.3 Mev

A 20.3 Mev gamma ray was obtained by bombarding a thick tritium target (B-127-1) with 800 Kev protons. Since these gamma rays are emitted in a $\sin^2$ distribution (Perry and Bame, 1955) both the scintillation counter with the $2\frac{1}{2}$"x$3\frac{1}{2}$" NaI crystal and the Mark I G-M counter were positioned at 90° to the proton beam. The scintillation counter face was 29.65 cm from the outside of the 2" diameter brass target pot while the G-M counter-to-target distance was varied from 5 cm. to 50 cm. The spectra obtained in the scintillation counter were similar to that in Figure 5. Counts were added in the spectra above the half-energy bias and an efficiency of 0.72 was assumed for this scintillation counter from a comparison of the $(1-e^{-\mu L})$ efficiencies of the two scintillation counters used throughout the work and the efficiency of the large crystal to the half energy bias taken from Figure 3. An effective centre distance of 3.6 cm. was also chosen on the same basis. The G-M counter efficiency was then obtained simply from $N_G = \frac{A\epsilon}{4\pi r^2} N_\gamma =$ $\frac{A\epsilon}{4\pi r^2} \frac{4\pi}{\Omega_s \epsilon_s} N_s$ where N_s was the number of counts to the half-energy bias in the 20 Mev spectrum and Ω_s, ϵ_s are the solid angle and efficiency respectively of the scintillation counter.

FIGURE 22 G-M COUNTER EFFICIENCY

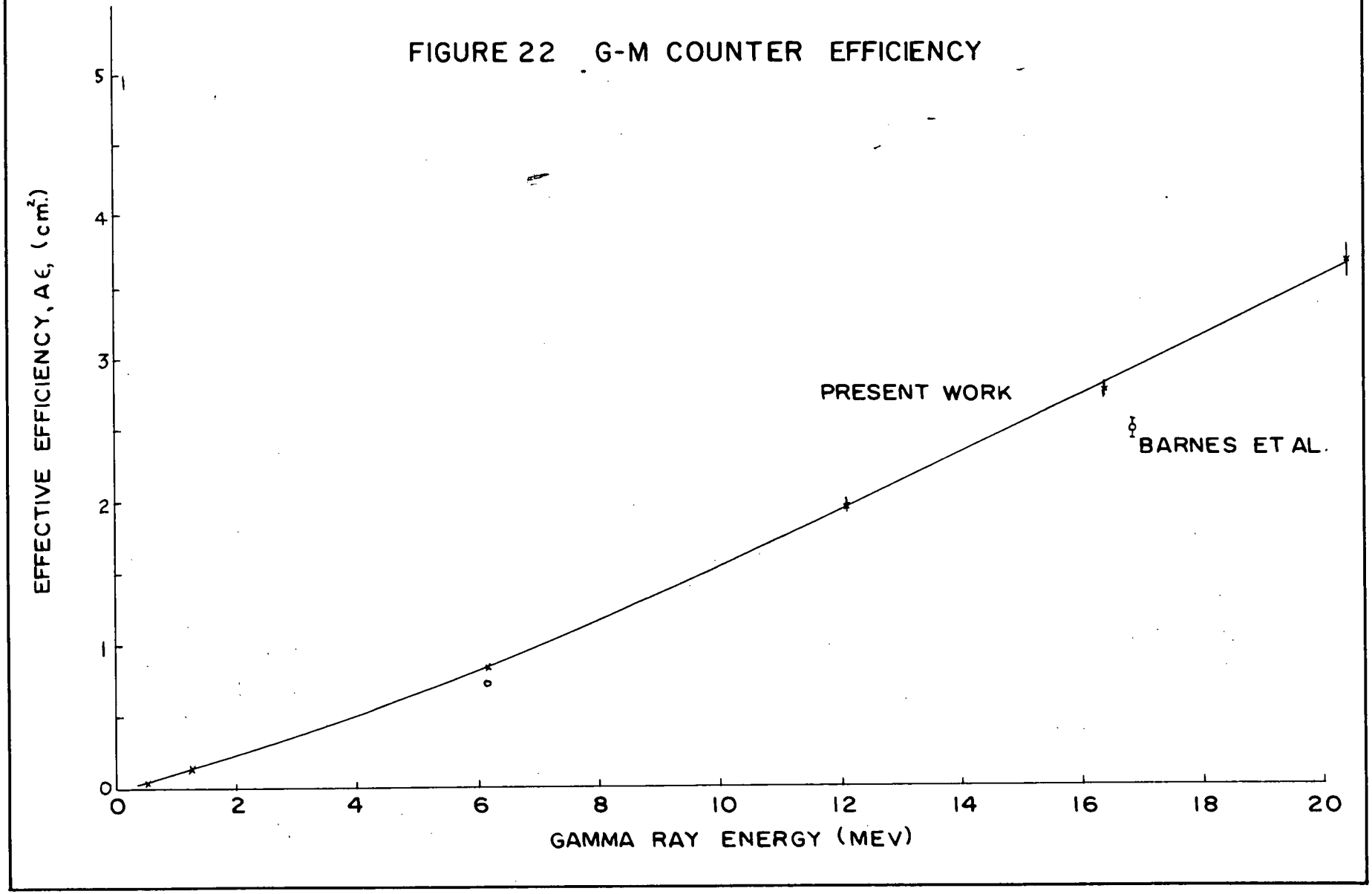

(i) Summary of Efficiency Results

The efficiencies are tabulated below. The statistical error shown in the fourth column does not include an error for the scintillation counter efficiency. Since a scintillation counter was used to determine the last three entries an uncertainty, considered to be 10% at the present time in the efficiency at energies over 12 Mev, should be added to the statistical error to give a total error estimate for these entries. For the first three entries the statistical error is to be taken as the total error.

E_γ (Mev)	$A\epsilon$ (cm^2) Mark I	$A\epsilon$ (cm^2) Mark II, No.1	Statistical Error
0.51	0.0444	0.0436	12%
1.25	0.138	0.146	0.8 %
6.16	0.845	0.787	2 %
12.1	1.97		3 %
16.3	2.77		2 %
20.3	3.68		3 %

To within the experimental error the effective centre occurs at the geometrical centre of the counter for all photon energies up to 20 Mev. These efficiency results are shown plotted in Figure 22. The smooth variation agrees with the results of Fowler et al. (1948). The two other points plotted are those of Barnes et al. (1952), the values being 0.73 ± 3%

at 6.13 Mev and 2.50 - 5% at 16.8 Mev. A rough curve drawn through the origin and these two points would have the same shape as the one found in this report thus lending confidence to the scintillation counter efficiency values in Figure 3.

Bibliography

Aaronson, D.A., 1950, M.A. Thesis, University of British Columbia.

Alkhazov, D.K., Grinberg, A.D., Lemburg, I. Kh., and Rozhdestvenskii, V.V., 1959, Soviet Physics, JETP, 36, 222

Ajzenberg, F., and Lauritsen, T., 1955, Rev. Mod. Phys. 27 77.

Barnes, C.A., Carver, J.H., Stafford, G.H., and Wilkinson, D.H., 1952, Phys. Rev. 86, 359.

Bleuler, E., and Goldsmith, G.J., 1952, "Experimental Nucleonics".

Bradt, H., Gugelot, P.C., Huben, O., Medicus, H., Preiswerk, P., and Scherren, P., 1946, Helv. Phys. Acta. 19, 77.

Breit, G., and Stehn, J.R., 1938, Phys. Rev. 53, 459.

Burbidge, E.M., Burbidge, G.R., Fowler, W.A., and Hoyle, F., 1957, Rev. Mod. Phys. 29, 559.

Devons, S., and Hine, M.G.N., 1949, Proc. Roy. Soc. (London) A199, 56.

Devons, S., and Lindsey, G.R., 1950, Proc. Phys. Soc. (London) 63A, 1202.

Dosso, H.W., 1957, M.A. Thesis, University of British Columbia.

v Droste, G., 1936, Zeits. fur Physik 100, 529.

Dunworth, J.V., 1940, Rev. Sci. Instr. 11, 167

Edwards, M., 1950, M.A. Thesis, University of British Columbia.

Fowler, W.A., 1958, Astrophys. J. 127, 551.

Fowler, W.A., Lauritsen, C.C., and Lauritsen, T., 1948, Rev. Mod. Phys. 20, 236.

Geiger, H., 1913, Verh. d. D. Phys. Ges., 15, 534, Phys. Zeits 14, 1129.

Geiger, H., and Klemperer, O., 1928, Zeits. fur Physik 49, 753.

Geiger, H., and Muller, W., 1928, Phys. Zeits, 29, 839.

Griffiths, G.M., Singh, P.P., Ssu, Y.I., and Warren, J.B., 1959, Can. Jour. Phys. 37, 1959.

Hanna, S.S., and Inglis, D.R., 1949, Phys. Rev. 75, 1767.

Holmgren, H.D., and Johnston, R.L., 1959, Phys. Rev. 113, 1556.

Kreger, W.E., 1954, Phys. Rev. 96, 1554.

Larson, E.A.G., 1957, M.A. Thesis, University of British Columbia.

Littauer, L.M., 1950, Proc. Phys. Soc. A63, 294.

Norling, F., 1941, Arkiv. Mat. Astron. Fysik 27A, 27.

Perry, Jr., J.E., and Bame, Jr., S.J., 1955, Phys. Rev. 99 1368.

Riley, P.J., 1958, M.A.Sc. Thesis, University of British Columbia.

Robertson, L.P., 1957, M.A. Thesis, University of British Columbia.

Rose, B., and Wilson, A.R.W., 1950, Phys. Rev. 78, 68.

Singh, P.P., 1959, Phd. Thesis, University of British Columbia.

Ssu, W., 1955, M.Sc. Thesis, University of British Columbia.

Walker, R.L., and McDaniel, B.D., 1948, Phys. Rev. 74, 315.

Whaling, W., 1958, Handbuch der Physik, Vol. 34, 193.

Whittaker, E.J., and Robinson, G., 1924, "The Calculus of Observations".